

1 Revisiting Neoproterozoic tectono-magmatic evolution of the northern
2 margin of the Yangtze Block, South China

3

4 **Peng Wu^{1,2}***, Yuan-Bao Wu³, Shao-Bing Zhang⁴, Yong-Fei Zheng⁴, Long Li⁵,
5 Ying Gao⁶, Hao Song^{1,2}, Zhengqi Xu^{1,2}, Zeming Shi^{1,2}

6

7 ¹*Applied Nuclear Technology in Geosciences Key Laboratory of Sichuan Province,
8 Chengdu University of Technology, Chengdu, Sichuan 610059, China*

9 ²*College of Earth Science, Chengdu University of Technology, 610059, China*

10 ³*State Key Laboratory of Geological Processes and Mineral Resources, Faculty of
11 Earth Sciences, China University of Geosciences, Wuhan 430074, China*

12 ⁴*CAS Key Laboratory of Crust-Mantle Materials and Environments, School of Earth
13 and Space Sciences, University of Science and Technology of China, Hefei 230026,
14 China*

15 ⁵*Department of Earth and Atmospheric Sciences, University of Alberta, Edmonton,
16 Alberta T6G 2E3, Canada*

17 ⁶*State Key Laboratory of Geohazard Prevention and Geoenvironment Protection,
18 College of Earth Sciences, Chengdu University of Technology, Sichuan 610059,
19 China.*

20

21 * Correspondence to pengwu@cdut.edu.cn (P. Wu)

22

23 **Abstract**

24 The Neoproterozoic tectonics of South China is crucial for understanding its
25 evolution history throughout the assembly and disintegration of Rodinia. Herein, we
26 employ integrally tectono-magmatic records over the period of ~1.0-0.6 Ga from the
27 northern Yangtze block, combining with available geochemical and geological data, to
28 investigate the secular tectonic evolution of the craton. Early Neoproterozoic intra-
29 oceanic subduction may have initiated at ~1.0-0.9 Ga after a long-period of late
30 Mesoproterozoic passive margin. A flare-up of magmatism at ~900 Ma attributed to
31 continental arc magmatism that led to increased crustal reworking during episodes of
32 arc compression and lithospheric thickening, and subsequently enhanced juvenile
33 mantle input during the transition to extensional back-arc rift modes. The isotope-
34 time pattern displays cyclic trends shifting towards less radiogenic values and then
35 progression to more radiogenic, near-depleted mantle isotope compositions, indicating
36 alternation regimes of contractional and extensional tectonics due to repeatedly slab
37 advancing and rollback. The occurrence of volumetrically-large radiogenic isotope-
38 depleted calc-alkaline rocks associations, low- $\delta^{18}\text{O}$ and bimodal rocks along the
39 Yangtze-block continental margin likely indicates rapid reworking of juvenile crust
40 within a composite tectonic setting involving both arcs and rifts, which may maintain
41 until the end of calc-alkaline arc magmatism at ~730-720 Ma and ultimately evolved
42 into an anorogenic rifted passive margin setting, as revealed by the deposition of
43 massive ~720-620 Ma syn-rift Yaolinghe-group volcanic-sedimentary sequence and
44 intraplate-like magmatism. Collectively, prolonged (~1.0-0.7 Ga) suprasubduction-
45 related magmatism traces accretion to the Yangtze-block margin, and thus likely
46 indicates a paleogeographically peripheral position of South China in Rodinia.

47

48 **Key words:**

49 Accretionary orogen, Rift magmatism, Tectono-magmatic evolution, Neoproterozoic,
50 Yangtze Block, Rodinia

51

52 **1. Introduction**

53 The South China Block, one of the largest Precambrian blocks in China, has
54 been considered as a key element in supercontinent Rodinia ([Zhao and Cawood, 2012](#); [Zhang and Zheng, 2013a](#); [Cawood et al., 2013](#)). However, the configuration of
55 Rodina remains controversial (e.g., [Li et al., 2008](#); [Evans, 2009](#)). Much of the
56 disagreement revolves around the paleogeographic position of South China in
57 Rodinia and whether it occupied an internal or peripheral location within the
58 supercontinent ([Cawood et al., 2013](#); [Li et al., 2008](#)), or whether it was even part of
59 Rodinia ([Merdith et al., 2017](#)). In reconstruction models favoring an internal location
60 within Rodinia, the South China has been invoked as providing a key link between
61 Laurentia and Australia (Missing-link, [Li et al., 1995](#)). The amalgamation of the
62 Cathaysia and Yangtze blocks is envisaged as occurring in an late Mesoproterozoic
63 to early Neoproterozoic Grenvillian collisional orogen (ca. 1000–890 Ma; [Li et al., 2007, 2009](#)), and is associated with the overall assembly of Laurentia and East
64 Australia-Antarctica, resulting in an united South China Block occupying an interior
65 position in an assembled Rodinia ([Li et al., 2014](#)). Subsequent breakout of South
66 China from this internal location is proposed to have involved pulses of bimodal
67 mantle plume magmatism between ~830–740 Ma and associated rift-related
68 sedimentation ([Li et al., 2003a, 2007](#)). In contrast, in models favoring an external
69 location for South China in Rodinia ([Zhao and Cawood, 1999](#)), assembly of the
70 Cathaysia and Yangtze blocks occurred in an overall accretionary orogenic setting
71 (e.g., [Wang et al., 2004, 2014](#); [Cawood et al., 2013](#); [Yao et al., 2016](#)). Final assembly
72 of the Yangtze and Cathaysia blocks was not complete until around 830–810 Ma and
73 subduction along the western margin of the Yangtze Block is inferred to have
74 continued until at least 730 Ma ([Zhou et al., 2002a,b](#); [Zhao et al., 2011](#)).

77 The two mutually exclusive models for the paleogeographic position of South
78 China in Rodinia have opposite consequences for the Neoproterozoic geological
79 history of South China. The former requires subduction to be completed by 890 Ma
80 ([Li et al., 2002](#); [Li et al., 2008](#)) or 860 Ma ([Shu and Charvet, 1996](#)) and subsequent

81 magmatism is related to lithospheric extension associated with a mantle superplume,
82 whereas the latter has subduction continuing until as late as 830–810 Ma on the
83 southeastern margin of Yangtze (Wang et al., 2006, 2007b, 2016c) and 730–720 Ma
84 on its northern to western margin (Zhou et al., 2002a,b; Dong et al., 2012). Thereby,
85 the source nature, age, petrogenesis and tectonic setting of the early to mid-
86 Neoproterozoic (ca. 1000–700 Ma) rocks in South China and in particular whether
87 they formed in an accretionary orogenic setting or an anorogenic setting are the key
88 in constraining the role of South China in the Rodinia cycle (Zhou et al., 2002a,b; Li
89 et al., 2003b,c; Zheng et al., 2007, 2008; Zhao et al., 2011).

90 In the past few decades, massive data, primarily focusing on geochronology,
91 geochemistry and petrogenesis of the Neoproterozoic igneous and sedimentary rocks
92 in South China, have been published. In recent years, many new data have been
93 available because of the development of in-situ analytical techniques. Despite the
94 numerous studies, the above issues continue to be debated. One of the most
95 important reason is the geochemical ambiguities, and thus allows for multiple non-
96 unique tectonic interpretations. More importantly, a critical evaluation and
97 integration of all available geological information, including paleomagnetism,
98 magmatism, metamorphism, lithostratigraphy and sedimentary provenance, remains
99 inadequate.

100 The northern Yangtze is a key area that preserves continuous tectono-magmatic
101 records including varying lithotypes with ages spanning ~1000-600 Ma, and thus is
102 ideal for determining and clarifying the secular evolution of South China during
103 Neoproterozoic. Herein, we mainly employ published whole-rock chemistry,
104 magmatic/detrital zircon U-Pb ages and Hf-O isotopes from both the igneous rocks
105 and sedimentary rocks from the northern Yangtze craton, and integrate available
106 regional metamorphism, tectono-stratigraphy and sedimentary provenance
107 information. The aim of this study is to explain the petrogenesis and tectonics of
108 magmatism on a large-scale time period rather than a specific individual pluton, or
109 we may lose the big picture. We finally outlined a revisited tectonic model and
110 highlight four tectonic stages: 1) intra-oceanic arc (~1000-900 Ma), 2) subsequent

111 flare-up of active continental margin arc magmatism and arc accretion (~890-830
112 Ma), 3) coexisting of continental arc and extensional intra-arc rift setting (~830?-730
113 Ma), and 4) rifted passive margin (~720-620 Ma). The paleogeographic position of
114 South China in Rodinia was also addressed.

115

116 **2. Geological characteristics of the northern Yangtze**

117 To fully address the geological characteristics of the Neoproterozoic rocks and
118 geological framework in the northern margin of the craton, we made a compilation of
119 published detrital zircon U-Pb-Lu-Hf isotopes of sedimentary rocks, magmatic zircon
120 U-Pb-Hf-O isotopes, and whole-rock chemistry of igneous rocks (except those from
121 the Dabie orogen where their Neoproterozoic protoliths suffered Triassic high-grade
122 metamorphism). To allow identification, we provide, where given in [Supplementary](#)
123 [Table S1-S5](#), original sample number, rock type, geologic unit, and location
124 description. We revalued some samples important to our interpretation; this was done
125 in particular for Chinese language papers, in cases of incomplete presentation (e.g.,
126 emphasis on a specific age group), or when we chose to highlight particular aspects of
127 the data that were not the focus of the original publication. In the following, we
128 describe the Neoproterozoic blocks/units/complexes identified in the northern margin
129 of the craton from west to east ([Fig. 1](#)), and provide an assessment of their tectono-
130 stratigraphy and magmatic-metamorphic evolution based on the integrated dataset.

131 **2.1 Bikou block and Mian-Lue complex**

132 The oldest crystalline basement (termed Yudongzi complex) exposes on the
133 northeastern edge of the Bikou block ([Fig. 1b](#)), consisting of ~2.8-2.5 Ga TTG gneiss,
134 granitic gneiss, amphibolite, chlorite schist, magnetite quartzite and has undergone
135 ~2.48, 1.85 Ga regional metamorphism ([Qin et al., 1992; Zhang et al., 2001; Zhang et](#)
136 [al., 2010; Zhou et al., 2018a; Zhang et al. 2020; Hui et al., 2017; Hui, 2021](#)). The
137 Bikou block comprises the Bikou and the Hengdan Groups and a series of intrusive
138 rocks. The Bikou Group is a volcano-sedimentary unit dominated by both arc-related
139 and intraplate-like spilite, basalt, basaltic andesite, dacite, and rhyolite ([Zhao et al.,](#)

140 1990; Yan et al., 2004a; Wang et al., 2008; Bader et al., 2013; Wu et al., 2019b).
141 Intrusive equivalents comprise a series of gabbro, diorite, granodiorite and quartz
142 monzonite that are linearly distributed along the NE-SW trending fault in the eastern
143 part of the Bikou block as lenses (Lai et al., 2007; Xiao et al., 2007; Ye et al., 2009;
144 Wang et al., 2012a; Gong et al., 2013; Ping et al., 2014; Hui et al., 2021), consistent
145 with the main structural stress direction (e.g., Pei, 1992). The Hengdan Group is a
146 typical suite of bathyal abyssal, pelagic to turbiditic, coarsening-upward (gravity-
147 flow) flysch sequence, consisting mainly of coarse-grained tuffaceous greywacke and
148 sandstone, with a small amount of phyllite and mud slate interbedded. These
149 sequences are generally weakly metamorphosed and still retain primary sedimentary
150 structures. Stratigraphic geochemical characteristics indicate that the Hengdan Group
151 was most likely deposited in a fore-arc basin (e.g., Druschke et al., 2006). New
152 detrital zircon U-Pb data constrain the maximum depositional age of the Hengdan
153 Group was at ca. 720 Ma (Gao et al., 2020; Hui et al., 2020b). The youngest rocks in
154 the Bikou block belong to a mafic dike swarm (~689 Ma; Yan et al., 2004a), which
155 probably formed in a rifted passive margin setting.

156 The Mian-Lue complex is situated at the northern edge of the Bikou block (Fig.
157 1b), composed predominantly of nappes with minor outcrops of ophiolitic blocks that
158 consists of low-grade serpentized harzburgite and minor dunite, amphibolite, gabbro,
159 metabasalt, basaltic andesite, and andesite, which shows multiple strongly ductile
160 shear deformation (Dong et al., 2011b). The ultramafic-mafic blocks, together with
161 marble, phyllite, schist and early Carboniferous radiolarian-bearing chert were termed
162 as the “Mianlue mélange”, which has been posited as a potential Phanerozoic suture
163 zone traversing the entire northern margin of the Yangtze craton based on the
164 conjectured existence of a Devonian-Permian “Mian-Lue ocean” (e.g., Meng and
165 Zhang, 1999, 2000; Lai et al., 2008). The primary evidence in support of this
166 hypothesis is the presence of ophiolitic blocks distributed along this suture zone, as
167 well as the occurrence of Middle-Late Paleozoic sediments (Lower Carboniferous,
168 Feng, 1996) in faulted contact with the ophiolites. The Triassic metamorphic (~220-
169 200 Ma) overprint has been interpreted as a consequence of the closure of the

170 Mianlue ocean. (e.g., [Li et al., 1996](#); [Zhang et al., 2002](#)). However, this hypothesis
171 was questionable, given that there are no ophiolites of matching age known along the
172 entirety of the Mian-Lue zone. Most of these metamorphic sedimentary rocks could
173 instead represent strata that record the Middle-Late Paleozoic subsidence of the
174 Yangtze passive margin (e.g., [Ratschbacher et al., 2004](#)). Recently zircon U-Pb dating
175 has revealed that these ophiolitic and arc-related rocks were formed during the early
176 Neoproterozoic (~985-800 Ma), rather than the Paleozoic ([Fig. 2a-b](#); [Zhang et al.,](#)
177 [2005](#); [Yan et al., 2007](#); [Wang et al., 2011](#); [Bader et al., 2013](#); [Lin et al., 2013](#); [Xu et al.,](#)
178 [2017](#); [Wu et al., 2019, 2021](#)).

179

180 **2.2 Micangshan-Hannan massifs**

181 The oldest crystalline basement of the Micangshan-Hannan massifs is
182 Paleoproterozoic Houhe complex (~2.08 Ga; [Wu et al., 2012](#)), which comprises
183 mainly migmatites, tonalitic/trondhjemite gneisses and minor amphibolites. The
184 unconformably overlying Huodiya Group consists mainly of marble dominated
185 Mawozi Formation (~1970 Ma, [Li et al., 2021a](#)) and the Shangliang Formation, and
186 was intruded by ~1.76 Ga A-type granites ([Deng et al., 2017, 2020](#); [Li et al., 2021a](#)).
187 The Tiechuanshan Formation was thought to belong to the upper sequence of the
188 Huodiya Group, and was dated at ~817 Ma ([Ling et al., 2003](#)), consistent with the
189 regionally upper amphibolite-facies metamorphism (~815 Ma, [Ling et al., 2006](#);
190 [Berkana et al., 2022](#)). The Neoproterozoic Xixiang-group strata exposed in the
191 Hannan region was originally subdivided into a hypometamorphic unit (the
192 Baimianxia, Sanwan, and Sanhuashi formations) and a epimetamorphic unit (the
193 Sunjiahe, Dashigou, and Sanlangpu formations) ([Tao et al., 1982](#)). Convincing
194 geochronological data yielded the formation ages of ~950-890 Ma for the Baimianxia
195 formation ([Ling et al., 2002, 2003](#); [Xu et al., 2009a](#)), ~845-833 Ma for the Sunjiahe
196 formation ([Zhao et al., 2006](#); [Xu et al., 2009b](#); [Cui et al., 2010, 2013](#)), ~803-776 Ma
197 for the Dashigou formation, and ~760 Ma for the Sanlangpu formation ([Xia et al.,](#)
198 [2009](#); [Deng et al., 2013a](#)). Alternatively, [Ling et al. \(2003\)](#) proposed that the Xixiang
199 Group could be further subdivided into the lower suite consisting of low-K basalts

200 and basaltic andesites, and the upper suite that composed of calc-alkaline to alkaline
201 basaltic andesites, dacites, and rhyolites. Volcanic and intrusive rocks (mostly
202 granitoids) in the Micangshan-Hannan massifs indicate a seemingly uninterrupted
203 magmatic activity spanning from ~0.96 to 0.72 Ga (Fig. 3b, Zhou et al., 2002a; Ling
204 et al., 2002, 2003, 2006; Zhao et al., 2006; Zhao and Zhou, 2008, 2009a, b; Liu et al.,
205 2009; Xia et al., 2009; Li, 2010; Geng, 2010; Zhao et al., 2010; Dong et al., 2011a,
206 2012; Cui et al., 2013; Ao 2015; Gan 2015; Wang et al., 2016a; Gan et al., 2017;
207 Duan et al., 2018; Luo et al., 2018; Zhou et al., 2018b; Zhu et al., 2018; Ao et al.,
208 2019; Wei et al., 2019; Hui et al., 2020a; Zhang et al., 2020).

209

210 **2.3 South Qinling Belt**

211 Minor gneisses and granulites within voluminous Triassic granitoids from the
212 Foping dome record a few ~2.5 and ~1.9 Ga inheritances of the South Qinling (Li et
213 al., 2000); Gneiss and schist of the Douling complex comprise the Neoarchean core
214 (~2.6-2.5 Ga) of the South Qinling (R.G.S. Henan, 1989; Zhang et al. 2004a, b; Zhang
215 et al. 2005; Hu et al., 2013; Wu et al., 2014; Nie et al., 2016). The Douling complex
216 underwent medium-grade regional amphibolite-facies metamorphism at ~820 and
217 ~780 Ma with peak metamorphic P-T conditions of 630-720°C and 8-11 kbar,
218 accompanied with a clockwise P-T path (Zhang et al., 1996; Hu et al., 2013, 2019;
219 Nie et al., 2016; He et al., 2020). Isotope characteristics and age suggest that their
220 protoliths are juvenile arc crust that formed at ~860 Ma (He et al., 2020). The Douling
221 complex was intruded by younger (~760-730 Ma) plutonic rocks (mostly gabbro to
222 granodiorite) (Fig. 2c; Xue et al. 1996; Chen et al. 2006b; Zhang et al. 2018; Bai et al.,
223 2019; Nie et al., 2019)

224 Early Neoproterozoic igneous rocks (~950-830 Ma; Liu, 2011; Liu et al. 2011,
225 2018; Yan et al. 2014; Hu et al. 2016; Zhang et al., 2016; Dong et al., 2017; Yang et
226 al., 2020; Cai et al., 2021; Wang et al., 2021; Yang, 2021) only exposed in the
227 northern margin of the South Qinling Belt (Fig. 2a-b). This magmatic belt stretches E-
228 W more than 200 km (Fig. 2b), likely defining the northernmost boundary of the
229 Yangtze craton (e.g., Mattauer et al., 1985). By comparison, the middle to late

230 Neoproterozoic volcano-sedimentary sequences and their intrusive equivalents are
231 widespread throughout the South Qinling belt (Fig. 2c-d). The volcano-sedimentary
232 sequences, mostly affected by greenschist-facies metamorphism, can be subdivided
233 into the Wudang, Yunxi, Suixian and Yaolinghe Groups.

234 The Wudang Group (Fig. 1b) comprises mainly of dacitic and rhyolitic tuff with
235 a small amount of basic and intermediate tuffs (Li and Zhu, 1930; R.G.S. Hubei,
236 1990). The Wudang Group that distributes in the Yunxi area was renamed as the
237 Yunxi Group, which is also referred to those volcano-sedimentary sequences that
238 expose in the Pingli and Niushan areas in southern Shaanxi Province (R.G.S. Shaanxi,
239 1989). Thus, the Wudang and Yunxi groups are actually synonymous. Geochronology
240 suggests that the age of the Wudang and Yunxi groups span 802-725 Ma (Li et al.,
241 2003a; Cai et al., 2006; Ling et al., 2007; Xia et al., 2008; Zhu et al., 2008; Yan et al.,
242 2010; Liu et al., 2020). The Suixian Group located to the southern side of the Tongbai
243 Mountains (Fig. 1b) consists mainly of schist, sandstone and meta-rhyolite layers
244 (HGB, 1982). Geochronology reveals that the Suixian Group was deposited during
245 ~760-720 Ma (Xue et al., 2011; Yang et al., 2016).

246 The Yaolinghe Group was originally named after the green-color meta-volcano-
247 sedimentary sequences in the Yaolinghe area of the Shangnan region (Fig. 1b; Yan,
248 1959), but now it generally refers to those greenschist-facies volcano-sedimentary
249 sequences that occupy a marginal location around the Wudang and Yunxi groups in
250 the Ankang-Piling-Wudangshan domes and contact with the underlying Wudang and
251 Yunxi groups by parallel unconformity and/or by ductile shear zone (e.g., Su et al.,
252 2006; Ling et al., 2007). Recent studies reveals that the so-called Yaolinghe-group
253 sequences exposed in the Zhen'an-Yaolinghe-Shangnan regions consist mainly of
254 early Neoproterozoic (~850 Ma) arc-like tholeiitic basalt and calc-alkaline andesitic to
255 rhyolitic rock associations with minor metasedimentary rocks (Li et al., 2003a; Bader
256 et al., 2013; Zhu et al., 2014; Yang, 2021; Zhao et al., 2022), whereas the late
257 Neoproterozoic Yaolinghe Group (637-641 Ma; Lan et al., 2022) outcropped in the
258 Niushan-Pingli-Wudangshan areas comprises mainly of tholeiitic basalts with a few
259 alkaline rhyolites (Cai et al., 2007; Ling et al., 2007, 2008; Xue, et al., 2011; Zhang et

260 al., 2013; Huang et al., 2021a; Wu et al., 2021b; Zhao et al., 2022). A number of mafic
261 dikes/sills and A-type granitic dikes were thought to be the intrusive equivalents of
262 the late Neoproterozoic within-plate volcanism (Hu et al. 2002; Niu et al. 2006; Wu,
263 et al., 2012; Wang et al., 2013, 2016b, 2017a,b; Guo et al., 2014; Shi and Deng, 2014;
264 Zhu et al., 2015; Deng et al., 2016; Li and Zhao, 2016; Liu and Zhang, 2018; Zhang et
265 al., 2018; Zhao and Asimow, 2018; Liu et al., 2022).

266

267 **2.4 Kongling Complex and Dahongshan**

268 The Kongling complex, exposed in the Huangling dome of the north interior of
269 the Yangtze Block, comprises volumetrically Archean rocks (Fig. 1b; Zhang et al.,
270 2006; Gao et al., 2011). High-grade metamorphism occurred at ~2.0 Ga (e.g., Wu et
271 al., 2009); post-orogenic granitoids intruded at ~1.85 Ga (e.g., Peng et al., 2012a).
272 The latest phase of magmatism in the Kongling area (termed Huangling pluton) was
273 at ~0.8 Ga (e.g., Zhang et al., 2008).

274 The late Meso- to early Neoproterozoic Miaowan ophiolite (Fig. 1b) located in
275 the southwestern Huangling dome, comprises amphibolite with pillow-lava relicts and
276 N-MORB tholeiitic chemistry, gabbro, diabase dikes, and ultramafic rocks (dunite,
277 harzburgite, podiform chromite) that formed at ~1.1-1.0 Ga (Peng et al., 2012b; Deng
278 et al., 2012, 2017). Dating of detrital zircons from the sedimentary unit and intruded
279 leucocratic veins of the Miaowan ophiolite constrains its emplacement age of ca. 900-
280 860 Ma (Lu et al., 2020).

281 In the Dahongshan area, southernmost of the Tongbai Mountain (Fig. 1b), the
282 Neoproterozoic Huashan Group is an angular unconformably overlain on the late
283 Mesoproterozoic Dagusi Group (~1.0 Ga, Huang et al., 2021b). The older (~970-840
284 Ma) felsic volcanic rocks, gabbros and granitoids display arc-like geochemical
285 affinities (Shi et al., 2007; Liao et al., 2016; Xu et al., 2016; Huang et al., 2023),
286 whilst the younger (~830-790 Ma) volcanic rocks and intrusives are bimodality and
287 show within-plate affinities (Deng et al., 2013c; Hu et al., 2015; Tian et al., 2017; Liu
288 and Zhao, 2019; Li et al., 2020; Liu et al., 2021; Huang et al., 2023). Detrital zircon
289 U-Pb dating places constraints on the maximum depositional ages of ~810-820 Ma

290 for the Huashan Group (Yang et al., 2018; Huang et al., 2021b).

291

292 **2.5 Tongbai–Hong’ an–Dabie**

293 The Tongbai-Hong’ an-Dabie orogen, the northeast part of the Yangtze Craton
294 (Fig. 1b), had been significantly reshaped due to the Mesozoic collision between the
295 North China Craton and the South China Block, resulting in multi-stage metamorphic
296 overprinting of the Precambrian rocks and strata. The Huangtuling complex is the
297 oldest crystalline basement of this region. Its protolith likely crystallized at ~2.70-
298 2.75 Ga and the granulite-facies (1.3 GPa, 850°C) overprint was at ~2.0 Ga (Chen et
299 al., 2006a; Wu et al., 2008), which is nearly coeval with the ~2.0 Ga metamorphism
300 in the Kongling complex. Numerous studies on the Triassic metamorphic rocks in the
301 Dabie orogen provide an understanding of their overwhelmingly Neoproterozoic meta-
302 igneous protoliths (Fig. 2); the protolith ages of gneisses cover ~950-582 Ma (median
303 at ~750 Ma, Fig. 3d). Most critically, positive zircon $\epsilon_{\text{Hf}}(t)$ and extensive low- $\delta^{18}\text{O}$
304 values suggest that their protoliths formed through rapid reworking of dominantly
305 juvenile crustal materials that had undergone high-T meteoric-hydrothermal alteration
306 (e.g., Yui et al., 1995; Ames et al., 1996; Rumble and Yui, 1998; Rumble et al., 2002;
307 Zheng et al., 2003, 2004, 2006, 2007; Wu et al., 2007; Fu et al., 2013; He et al., 2016,
308 2018).

309

310 **3. Discussion**

311 **3.1. Protracted subduction accretion**

312 **3.1.1 Early Neoproterozoic intra-oceanic subduction**

313 Rarely exposed Late Mesoproterozoic rocks in South China have traditionally
314 been thought to mark Grenvillian orogens and are widely used for reconstruction of
315 Rodinia (e.g., Li et al., 2008). However, petrological and geochemical investigations
316 on these rocks, such as the ca. 1020 Ma mafic dykes and A-type granitoids in the
317 Tianbaoshan Formation of the Huili Group (Zhu et al., 2016; Wang et al., 2019a,c),

318 the ca. 1140 Ma alkali basalts in the Laowushan Formation on the western margin of
319 the Yangtze craton (Greentree et al., 2006), and the ca. 1159 Ma Tieshajie bimodal
320 volcanic rocks (Li et al., 2013b) on the southeastern margin of the craton, indicate
321 formation in a rifting setting. Additionally, detrital zircon U-Pb-Hf-O isotopes and
322 stratigraphical studies on the late Mesoproterozoic sedimentary sequences on the
323 peripheries of the craton, such as the Kunyang, Huili and Julin Groups in the western
324 margin, and the Shennongjia and Dagushi groups in the northern margin (e.g., Sun et
325 al., 2009; Qiu et al., 2011; Li et al., 2013a; Du et al., 2016), suggest a stable passive
326 continental margin setting, arguing against existence of the so-called Grenvillian
327 collisional orogen in South China.

328 Nevertheless, stratigraphical and provenance studies on the Huili and Julin
329 sequences also imply a transition from a passive margin to a convergent continental
330 margin setting (e.g., Sun et al., 2022), which is consistent with the observations of
331 fold deformations developed in the late Mesoproterozoic Dagushi Group and the
332 overlying Huashan Group in the Dahongshan area. These fold deformations are
333 interpreted to be attributed to early Neoproterozoic subduction-related tectonic
334 compression events (Huang et al., 2021b). Although how the tectonic switching from
335 the late Mesoproterozoic rifted passive margin to the early Neoproterozoic convergent
336 active continental margin is still controversial, the occurrence of ~1.0-0.9 Ga arc
337 rocks and associated ophiolites within and/or around the craton indicates the remnants
338 of fossil subducted oceanic lithosphere of the circum-Yangtze subduction (e.g., Deng
339 et al., 2012, 2017; Hu et al., 2017). To date, chronology suggests the ages of intra-
340 oceanic arc magmatism range from ~985 to 900 Ma (e.g., Li et al., 2009; Li et al.,
341 2018a; Wu et al., 2019, 2021; Huang et al., 2023), suggesting that the initiation timing
342 and duration of intra-oceanic subduction could be variable in different areas of the
343 Yangtze craton. These island arc magmatic activities may be diachronous- since they
344 have been formed in an identical subduction-related tectono-magmatic setting around
345 the Yangtze craton, but through different time (Li et al., 2021a). The ~1.0-0.9 Ga arc
346 rocks have strongly positive zircon $\epsilon_{\text{Hf}}(t)$ values, mantle-like zircon $\delta^{18}\text{O}$ values (Fig.
347 4) and relatively low concentrations of highly incompatible trace elements compared

348 to the average upper continental crust ([Rudnick and Gao, 2003](#)), which are similar to
349 the juvenile arc lavas from the modern IBM island arc, and further suggestive of an
350 intra-oceanic subduction origin (e.g., [Li et al., 2009, 2018a; Wu et al., 2019, 2021](#)).

351 **3.1.2 From intra-oceanic subduction to ocean-continent subduction**

352 Published geochronological data coverage shows that <0.9 Ga arc rocks are
353 widespread throughout the northern Yangtze ([Fig. 2b](#)), likely indicates a flare-up of
354 continental arc magmatism along the Yangtze-block continental margin. The possible
355 tectonic transition from ocean-ocean subduction to ocean-continent subduction are
356 supported by the following evidences: 1) Rarely exposed 1.0-0.9 Ga island arc rocks
357 suggest only a few were survived from being subducted or accretionary erosion; 2)
358 the 1.0-0.9 Ga arc rocks are geochemically low- to mid-K series ([Fig. 5](#)) and have
359 relatively low concentrations of highly incompatible trace elements ([Fig. 6](#)), similar to
360 the geochemical affinities of the modern island arc rocks (e.g., Izu-Bonin-Mariana,
361 [Saito and Tani, 2017](#)), whilst the post-0.9 Ga arc rocks have pronounced enrichment
362 of LILEs and LREEs ([Fig. 6](#)), resembling the composition of the mature continental
363 crust; 3) The 1.0-0.9 Ga arc rocks have little ancient inherited zircons and are
364 isotopically characterized by strongly positive whole-rock $\epsilon_{\text{Nd}}(t)$, zircon $\epsilon_{\text{Hf}}(t)$ values
365 and mantle-like zircon $\delta^{18}\text{O}$ values, while the post-900 Ma arc rocks show stronger
366 continental reworking with less radiogenic isotopes and elevated zircon $\delta^{18}\text{O}$ values
367 ([Fig. 4](#)); 4) The sharp change of detrital zircon Hf-O isotopes may reflect the tectonic
368 switching, i.e., detritus zircons with ages of ca. 970-900 Ma from the Miaowan fore-
369 arc metasedimentary have mantle-like zircon $\delta^{18}\text{O}$ (4.5–6.0‰) and high $\epsilon_{\text{Hf}}(t)$ values
370 (up to +14), whereas some 900 Ma detrital zircons low $\epsilon_{\text{Hf}}(t)$ values (-6~ -33) and
371 high $\delta^{18}\text{O}$ values (6.5-9.2‰), indicating incorporation of recycled supracrustal
372 materials into the sources ([Lu et al., 2020](#)). Similarly, detrital zircon Hf isotopes of the
373 Huashan Group in the Dahongshan area also show a sharp decrease at ~900-880 Ma
374 (from +13.5 to -18.5, [Huang et al., 2021b](#)), which is interpreted as the tectonic
375 transition from island arc to continental arc; 5) The emplacement of ~890-860 Ma

376 alkaline intrusive rocks aligning with an EW trend paralleled to the fossil subduction
377 zone in the innermost of the Micangshan massif (Gan et al., 2017), which were likely
378 formed in a local extensional setting caused by roll-back of the slab that had
379 subducted underneath the Yangtze continental margin (Zhou et al., 2018b). In
380 summary, an integral geochronological, geochemical and isotopic evidences for
381 igneous rocks and sedimentary provenance herald the tectonic switch from island arc
382 to continental arc at ~900-880 Ma, which manifests enhanced crustal reworking and
383 the change of magma source via incorporation of more continental clastic components
384 into the ocean-continent subduction channel along the Yangtze-block margin.

385 **3.1.3 Periodically extensional and contractional tectonics**

386 Generally, an accretionary orogen can undergo multiple cycles of tectonic mode
387 switching (e.g., Lister et al., 2001; Collins and Richards, 2008; Kemp et al., 2009).
388 However, the prolonged accretionary history of the northern margin of the Yangtze
389 block has not been well understood yet. Here, we address this issue by employing the
390 distinctive archive of oxygen and hafnium isotopes in igneous rock-hosted zircon
391 from the northern Yangtze. Because zircon-hosted isotope tracer information has
392 potential for evaluating relative contributions from mantle and crustal sources (Kemp
393 et al., 2007; Yang et al., 2007), and thus for monitoring tectonic mode alternation
394 during magmatic episodes.

395 The published zircon Hf-O isotope compositions of Neoproterozoic igneous
396 rocks from the northern Yangtze are illustrated in [Supplementary Table S3](#) and [S4](#).
397 When plotted as a function of crystallization age, the zircon Hf and O isotope data
398 define striking temporal trends. During 0.9-0.8 Ga, the ϵ_{Hf} -time pattern of magmatism
399 from the northern Yangtze shows an overall at least two abrupt decreases (~870 Ma
400 and ~830 Ma) and then approach depleted mantle-like values ([Fig. 4](#)). The zircon
401 $\delta^{18}\text{O}$ -time patterns change from mantle-like $\delta^{18}\text{O}$ values to progressively elevated
402 during ~900-830 Ma, and then downward to mantle-like or sub-mantle values for the
403 post-830 Ma igneous rocks ([Fig. 4](#)). The similar $\delta^{18}\text{O}$ -time pattern and “W-shaped”

404 ϵ_{Hf} -time pattern are duplicated in different regions of the northern Yangtze, such as
405 the Mian-Lue-Bikou, Dahonshan, Hannan-Micangshan and the South Qinling, likely
406 indicates consistent tectonic dynamic processes along the northern margin of the
407 craton during the prolonged accretionary orogenesis.

408 Tectonic mode switching appears capable of reconciling the complex isotope-time patterns defined by the northern Yangtze magmatic rocks. In this scenario, trends
409 towards decreasing $\epsilon_{\text{Hf}}(t)$ values and elevated $\delta^{18}\text{O}$ values reflect enhanced crustal
410 reworking attending arc compression and lithospheric thickening. Enhanced crustal
411 input could have occurred by increased sediment subduction, greater subduction
412 erosion and delivering more supracrustal materials to the mantle source, or various
413 contamination with ancient continental basement materials during the magmas
414 passage through the thickened crust. However, the subsequent progression to juvenile
415 isotope signatures manifests enhanced mantle input as switching to an extensional
416 mode induced by the re-initiation of subduction retreat. In particular, the episodically
417 emplaced A-type rocks and associated mafic-ultramafic rocks with intraplate-like
418 geochemical affinities (e.g., [Ling et al., 2002](#); [Gan et al., 2017](#); [Luo et al., 2018](#); [Zhou et al., 2018b, 2019](#); [Ao et al., 2019](#); [Wei et al., 2019](#); [Wu et al., 2019b](#)) are evidently
420 controlled by the continental back-arc rifts, which in turn is linked to periodically slab
421 rollback. The transition in geochemistry from arc-like to intraplate-like reflects a
422 diminishing subduction-induced enrichment in the mantle source as switching to
423 extensional episodes. Collectively, the repeated isotope-time enriching and depleting
424 variations of igneous rocks was proposed to correlate with the alternating regimes of
425 contractional and extensional tectonics of a prolonged active continental margin
426 developed along the northern margin of the Yangtze craton, and suggest a long term
427 feedback between tectonic activities and magma source during Neoproterozoic (e.g.,
428 [Wu et al., 2023](#)).
429

430
431 **3.2 Rift-related magmatism revisited**

432 **3.2.1 Early Neoproterozoic localized rifting during arc accretion**

433 The origin and tectonic setting of early Neoproterozoic rift-related magmatism
434 are still controversial. Zhou et al. (2019) reported ca. 900 Ma low- $\delta^{18}\text{O}$ A-type
435 rhyolite from the Tongbai area of the northern Yangtze, and interpreted that they were
436 formed in a back-arc rift setting in an accretionary orogen. In contrast, Zhou et al.
437 (2018) reported a series of ca. 900-890 Ma mafic intrusions and alkaline complexes
438 with intraplate-like geochemical affinities from the innermost Micangshan area, and
439 proposed that they may mark the onset of continental rifting or the ending of Late
440 Mesoproterozoic to Early Neoproterozoic lithospheric extension. However, another
441 episode of alkaline intrusives (ca. 870-860 Ma; Gan et al., 2017) in the same area,
442 contemporaneous with the ca. 865-860 Ma Wangcang alkaline, tholeiitic and high-Nb
443 volcanism, were considered to be formed in an extensional back-arc setting (Berkana
444 et al., 2022). The ca. 860 Ma arc-like tholeiitic mafic sills in the same Micangshan
445 area were suggested to be generated by partial melting of a metasomatized mantle
446 wedge, which further supports a continental back-arc setting (Hui et al., 2020a).
447 Besides, the occurrence of ca. 850-850 Ma intraplate-like mafic intrusives and high-
448 Mg diorites from the Xiaomoling complex of the South Qinling Belt (Wu et al.,
449 2023), and ca. 830 Ma low- $\delta^{18}\text{O}$ A-type rhyolites from the Dahongshan area of the
450 northern Yangtze (Huang et al., 2023) also support a local back-arc rift origin during
451 the early Neoproterozoic subduction accretionary orogen. Therefore, the temporally
452 continuous but spatially dispersed early Neoproterozoic rift-related (or intraplate-like)
453 magmatic activities (Fig. 7) are most likely indicative of localized back-arc rifting
454 environment induced by periodic subduction retreat in a prolonged accretionary
455 orogen along the northern Yangtze as discussed in section 3.1.

456 **3.2.2 Origin of post-830 Ma rocks: Anorogenic magmatism?**

457 Widespread mid-Neoproterozoic rift magmatism and rifting-basin sequences in
458 South China are traditionally considered the products of anorogenic magmatism in
459 intracontinental rift basins related to mantle plume activity during the breakup of

460 Rodinia (Li et al., 2008, and references therein), and thus supporting the “internal
461 model” for the position of South China in the configuration of Rodinia (Li et al., 2008
462 and references therein). Plume-rift model further proposed that continental rift
463 magmatism has initiated since ca. 830 Ma (or even earlier at ca. 860 Ma, Li et al.,
464 2003b). Supporting evidences include: (1) the ca. 830 Ma mafic to ultramafic dykes
465 and sills in South China are identical in age to the Gairdner Dyke Swarm in Australia
466 (Li et al., 1999), (2) the ca. 825 Ma Yiyang komatiitic basalts were considered the
467 products of mantle plume (Wang et al., 2007a), and a few ca. 820-810 Ma basalts with
468 intraplate-like affinities from the Bikou Group and the Tiechuanshan Formation were
469 regarded as the remnants of flood basalt (e.g., Li et al., 2002; Ling et al., 2003; Wang
470 et al., 2008; Wu et al., 2019b); (3) the regionally unconformity between the Banxi
471 Group and Lengjiaxi Group were interpreted as continent-scale doming and unroofing
472 due to underplating of plume head; (4) The stratigraphic characteristics and
473 provenance record of the Neoproterozoic rift basin (Nanhua and Kangdian) have also
474 been used to support internal models for the position of South China (Li et al., 2002,
475 2003a). Proponents of the internal model suggest extension was associated with a
476 “superplume” that cause the breakup of Rodinia and correlates with contemporaneous
477 rift systems in eastern Australia and western Laurentia (Li et al., 2008). Thus the
478 Nanhua sequences and equivalents (e.g., Kangdian sequences) represent sediment
479 accumulation during lithospheric extension (Wang and Li, 2003).

480 Authors that argued against the “plume-rift” hypothesis demonstrate that
481 sedimentary detritus supplied to the Nanhua Basin sequences were largely sourced
482 from Neoproterozoic rocks within South China based on U-Pb age patterns and Hf
483 isotopic signatures of detrital zircons from the Danzhou, Xiajiang and Banxi groups
484 (Wang and Zhou, 2012; Wang et al., 2012b). The absence of late Mesoproterozoic
485 aged detritus as well as only minor input from Archean and Paleoproterozoic cratonic
486 sources in the Nanhua sequences is distinct from the detrital age patterns of time-
487 equivalent strata in Laurentia and Australia, but is similar to that of Cryogenian strata
488 in the Lesser Himalaya of northwest India (Hofmann et al., 2011). Specifically, flood
489 basalts related to the inferred ‘super-plume’ are documented in Australia but are not

490 present in the Yangtze Block. Although [Li et al. \(1999\)](#) suggests that the absence of
491 flood basalts in South China may have been attributed to erosion during
492 sedimentation of the Neoproterozoic sedimentary basins, similar to that occurred in
493 the Adelaide Fold Belt in Australia ([Barovich and Foden, 2000](#)) However,
494 sedimentary rocks from the Nanhua sequences have trace elemental and Sm-Nd
495 isotopic signatures indicative of sources dominantly composed of granitic to dioritic
496 end-members from the interior of the Yangtze Block ([Xu et al., 2007; Wang and Zhou,](#)
497 [2012](#)), arguing against derivation of sedimentary detritus from a flood basalt province.
498 Besides, stratigraphical studies suggest that the Hengdan Group in the Bikou block
499 was deposited in a fore-arc setting at ca. 720 Ma ([Druschke et al., 2006; Gao et al.,](#)
500 [2020; Hui et al., 2020b](#)), and continuously received clastic materials from the early to
501 mid-Neoproterozoic magmatic detritus.

502 On the other hand, the occurrence of voluminous mid-Neoproterozoic calc-
503 alkaline rock assemblages characterized by hornblende-rich lithologies (mostly diorite
504 and granitoids) along the northern and northwestern margins of the Yangtze craton
505 ([Fig. 7](#)) cannot be reconciled with the anorogenic magmatism induced by a mantle
506 superplume activity. Because it seems highly unlikely that the calc-alkaline rock
507 associations are dominant lithotypes rather than the flood basalts and bimodal
508 volcanics in a typical intracontinental rift, i.e., the Main Ethiopian rift of the East
509 African rift system and the Iceland rift (e.g., [Corti, 2009](#)). The typical calc-alkaline
510 rock associations are widespread in the northern to western Yangtze, including the ca.
511 750-730 Ma Fenghuangshan dioritic-granitic plutons, the ca. 730 Ma Gangou
512 gabbroic-granitic plutons in the Douling batholith (e.g., [Wang et al., 2019b](#)), the ca.
513 760 Ma Xixiang hornblende-rich diorite ([Zhao et al., 2010](#)) and a series of ca. 810-
514 730 Ma adakitic tonalite-trondhjemite and associated granitic plutons, such as the
515 Erliba-Wudumen plutons in the Hannan batholith and the Xielongbao, Shimian, Yele,
516 Mopanshan, Dajianshan and Datian plutons from the western Yangtze ([Zhao and](#)
517 [Zhou, 2008; Zhao et al., 2021](#)). Detailed petrological, bulk-rock and mineral
518 geochemical and O–Hf–Nd isotopic studies suggest that these ~800-730 Ma calc-
519 alkaline granitoid associations were most probably generated through partial melting

520 of hydrated basaltic rocks in the arc root, and thus support a continental arc setting
521 (e.g., [Zhao et al., 2021](#)).

522 Despite the two mutually exclusive models (slab-arc vs. plume-rift), a reconciled
523 “plate-rift” model proposed by [Zheng et al. \(2007, 2008\)](#) emphasizes the 830–800 Ma
524 magmatism as the product of the orogenic collapse of an arc-continent collisional
525 orogen rather than a superplume that led to the breakup of Rodinia, and suggests that
526 the whole South China experienced lithospheric extension and intracontinental rifting
527 during ~780–740 Ma due to mantle upwelling and concomitant orogenic collapse that
528 may have triggered supercontinent break-up and associated syn-rift magmatism.
529 However, The plate-rift model is based on a systematic study of zircon U–Pb and Lu–
530 Hf isotopes and whole-rock Sr–Nd isotopes for the Neoproterozoic volcanic rocks and
531 granitoids from the eastern part of the Jiangnan Belt, whether it can apply for
532 interpreting the tectonic evolution of the northern-Yangtze magmatism needs to be
533 further verified and examined.

534 **3.2.3 Mid-Neoproterozoic magmatism revisited: rifts superposed on continental
535 arc**

536 Thus far, a paucity of exact petrological and geological documentation exists
537 pertaining to plume-related magmatic activity (episodic and short duration, ~1–5
538 m·yr). Alternatively, an abundance of petrological, geochemical and geological
539 evidences for the slab-arc model (a long-lived active convergent margin) are the most
540 persuasive among other models especially for those igneous rocks from the northern
541 to western Yangtze (e.g., [Zhou et al., 2002a,b, 2006a,b; Zhao and Zhou, 2009b; Zhao](#)
542 [et al., 2011, 2021; Luo et al., 2018; Wang et al., 2019b; Zhao et al., 2021](#)).

543 Nevertheless, oxygen isotope data coverage ([Fig. 4h](#)) reveals that continental-scale
544 rift magmatism appears to have been most active at ca. 780–750 Ma. An abundance of
545 post-800 Ma low- $\delta^{18}\text{O}$ igneous rocks and associated A-type granitoids and bimodal
546 volcanism were identified in the northern, western and southeastern margin of the
547 Yangtze craton (e.g., [Lu et al. 1999; Wang et al., 2009, 2010; Zhang and Zheng,](#)

548 2013b; Zou et al., 2021), providing compelling support for tectonic interpretations
549 positing that the middle Neoproterozoic rift-related magmatism likely emerged within
550 craton-scale continental rifts, probably coinciding with the breakup of Rodinia.
551 However, the occurrence of voluminous ~800-730 Ma calc-alkaline rock associations
552 consisting of hornblende-rich gabbro, diorite, tonalite, and granodiorite in the
553 northern and western margin of the Yangtze craton indicates unlikely an anorogenic
554 tectonic setting, because typical anorogenic intracontinental rifts produce
555 predominately flood basalts and bimodal volcanic lithologies rather than calc-alkaline
556 rocks associations (e.g., Corti, 2009). Specifically, most of the ~800-730 Ma igneous
557 rocks are characterized by juvenile isotope signatures such as positive whole-rock
558 $\varepsilon_{\text{Nd}}(t)$ and zircon $\varepsilon_{\text{Hf}}(t)$ values, suggesting rapid reworking of juvenile crustal materials.
559 Collectively, we propose a composite tectonic setting involving both intra-arc rift and
560 continental arc may have existed along the periphery of the Yangtze craton during
561 ~800-730 Ma. Such composite tectonic regime was also observed in the early
562 Mesozoic to Cenozoic Cordillera Orogen, where intra-arc rifts co-exist with the
563 protracted continental arc during the subduction of (proto-) pacific slab (e.g., Lawton
564 and McMillan, 1999; Rapela et al., 2005).

565 This composite tectonic setting can self-consistently well explains the origin of
566 both voluminous calc-alkaline and bimodal rock associations fingerprinted with ^{18}O -
567 depletion signatures. Since crustal fingerprinting by low $\delta^{18}\text{O}$ meteoric/glacial water
568 may be accomplished via tectonically induced water-rock interaction during
569 syngenetic rifting and alteration along normal faults (e.g., Bindeman and Simakin,
570 2014). Rifting and burial due to extension in turn create additional hydrogeological
571 conditions for hydrothermal fluid circulation. Conditions for remelting may be
572 optimized when the low $\delta^{18}\text{O}$ protoliths are brought down closer to the heat source
573 during crustal burial processes. Such crustal burial processes may have enhanced by
574 rapid endogenic recycling process in the intra-continental arc thrust faults (e.g.,
575 DeCelles et al., 2009; Sauer et al., 2017; Pearson et al., 2018; Li et al., 2021b).
576 Therefore low- $\delta^{18}\text{O}$ protoliths formed through high-temperature hydrothermal
577 alteration in upper-crust rifts or normal faults can potentially and efficiently be

578 transported into the lower crust depth where partial melting taking place and
579 producing massive low- $\delta^{18}\text{O}$ magmas (Fig. 2c). According to the estimates of the
580 maximum burial rates of ~4 mm/yr (Sauer et al., 2017), the time scale for supracrustal
581 materials transporting into the ~30 km-depth crustal level is less than ~8 Ma. This
582 time is even shorten for the low- $\delta^{18}\text{O}$ protoliths because they could have formed in the
583 deep compared to the supracrustal materials. Thus the time interval is less or in the
584 range of analytical error of SIMS or LA-ICPMS zircon U-Pb dating for the
585 Precambrian rocks. Consequently, it seems that the Neoproterozoic low- $\delta^{18}\text{O}$
586 magmatic rocks were formed through cannibalization or remelting of syn-
587 magmatically altered rocks during syngenetic rift hydrothermal alteration and magma
588 pulse (e.g., He et al., 2018). Taking together, we hence proposed that the ca. 830–730
589 Ma rocks in South China are most likely formed in a composite tectonic setting rather
590 than a single tectonic environment. This setting likely involved the presence of both
591 continental rifts and continental arcs, though in different regions the things might be
592 different.

593 **3.2.4 Late Neoproterozoic rifted passive margin**

594 The calc-alkaline magmatism ended at approximately 730-720 Ma (Nie et al.,
595 2019; Wang et al., 2019b), likely indicates the end of continental arc setting along the
596 northern to western margin of the Yangtze craton. Chronology reflects that the post-
597 720 Ma magmatism can last until ~620 Ma, with mostly exposed in the South Qinling
598 Belt (Fig. 2d and Fig. 3c), as is representative of the Yaolinghe-group volcanism. This
599 late Neoproterozoic volcanoclastic sequence is of more than 1,200 m in thickness and
600 was considered to have formed in an intracontinental rift basin (e.g., Ling et al., 2008)
601 or a passive continental rifted margin (insert in Fig. 2d; Zhao and Asimow, 2018).
602 New high-precise chronology reveals that the Yaolinghe-group volcanism erupted at
603 637-641 Ma (CA-ID-IRMS, Lan et al., 2022), 2–6 Myr before the termination of the
604 Marinoan glaciation. An early stage of large magmatic province (~720-717 Ma) prior
605 to the initiation of the Sturtian snowball has also been identified, which is interpreted

as relating to the Franklin-aged mantle superplume beneath supercontinent Rodinia (Lu et al., 2022). Besides, there are several small-scale magmatic pulses between the ~720-620 Ma, such as the ca. 690-680 Ma and the ca. 660-650 Ma volcanism and equivalent intrusives (e.g., Niu et al., 2006; Ling et al., 2007; Zhu et al., 2008, 2015; Lan et al., 2015a,b; Zhao and Asimov, 2018; Liu et al., 2022; Zhao et al., 2022). Geochemical compositionally, the ~720-620 Ma magmatism that can be attributed more clearly to intraplate-like and bimodal magmatism compared to that of the pre-720 magmatic rocks (Fig. 5 and 6). The tholeiitic basalts and mafic-ultramafic sills range from MORB-type to OIB-type trace element patterns, while the acid end-member (mostly granite and rhyolite) showing clear A-type affinities with strongly enrichment of LILEs and HFSEs and depletion of Sr, Ti and Y contents (Fig. 6). In Th/Yb versus Ta/Yb (Fig. S1) and the Nb versus Y diagrams (Fig. S2), both the A-type rocks and mafic rocks were plotted in the within-plate field. Besides, the generation of low- $\delta^{18}\text{O}$ felsic volcanic rocks and intrusive equivalents during this period (e.g., Liu and Zhang, 2013; Yang et al., 2016; Liu and Zhang, 2018) suggests that intracontinental rifts were widely developed along the periphery of the Yangtze craton accompanied with the continuous extensional tectonic setting due to the breakup of Rodinia. Collectively, the ^{18}O -depletion signatures, bimodality and intraplate-like geochemical affinities strongly indicate that the late Neoproterozoic (ca. 720-620 Ma) magmatism in the northern Yangtze were formed in a typical rifted passive margin setting.

627

628 **4. Implication to South China locating in Rodinia**

629 The paleogeographic location of South China within the supercontinent Rodinia
630 has been hotly debated (e.g., Li et al., 2008; Evans, 2009; Cawood et al., 2013, 2018).
631 Traditionally, South China was considered to situate at low latitudes between
632 Laurentia and Australia (Li et al., 1995). However, new reliable paleomagnetic
633 data propose that South China was either completely disconnected from Rodinia or
634 located at its periphery between ~1000 to 720 Ma (Jing et al., 2015, 2019, 2021; Niu

635 et al., 2016; Park et al., 2021; Xian et al., 2020; Chang et al., 2022; Fu et al., 2022).
636 This is consistent with the prolonged subduction accretion in South China during
637 early to middle Neoproterozoic (~1000-730 Ma, Fig. 2a-d), which cannot be
638 reconciled with a position of South China within the interior of a stable
639 supercontinent anytime in the Tonian Period. Besides, synchronous Neoproterozoic
640 low $\delta^{18}\text{O}$ magmatism occurred in South China, NW India (Wang et al., 2017),
641 Madagascar (Archibald et al., 2016) and Seychelles (Harris and Ashwal, 2002)
642 suggests a close linkage among these blocks during the Rodinia breakup (e.g., Huang
643 et al., 2019; Wu et al., 2020). This was supported by the similar provenance records of
644 the late Neoproterozoic to Paleozoic passive margin clastic sequences from both the
645 South China and India (Hofmann et al., 2011), implying their proximity along the
646 same passive margin during the break-up of Rodinia. Collectively, an integration of
647 key data sets such as paleomagnetism, geology and tectono-stratigraphy indicates that
648 South China was unlikely to have occupied a central position in Rodinia (Fig. 8).

649

650 **5. Conclusions**

651 1. The initiation of intra-oceanic subduction along the periphery of Yangtze was
652 diachronous during ca. 1000-900 Ma, followed by the flare-up of active continental
653 margin arc magmatism at ca. 900-880 Ma.

654 2. Repeatedly variants of isotopic compositions of igneous rocks reveal the
655 alternating regimes of contractional and extensional tectonics during the early
656 Neoproterozoic arc accretion. The episodically occurrence of A-type, intraplate-like
657 and low- $\delta^{18}\text{O}$ magmatism during this period marks the transition of tectonic switching
658 to extensional modes due to the retreat of subduction.

659 4. Massive radiogenic isotope-depleted calc-alkaline rock associations, low- $\delta^{18}\text{O}$
660 and bimodal volcanism exposed along the Yangtze-craton margin may formed in a
661 composite tectonic setting that involves both continental arc and rift settings. The end
662 of arc magmatism was marked by the termination of calc-alkaline magmatism at
663 ~730-720 Ma prior to the onset of the Sturtian glaciation.

664 5. The ~720-620 Ma magmatism formed in the intra-continental rifts of the
665 volcanic passive margin setting.

666 6. South China is likely peripheral or disconnected from Rodinia.

667

668 **Data Availability Statement**

669 All data are available at the following link <https://doi.org/XXXX.figshare.XXX>

670

671 **Acknowledgement**

672 This work was financially supported by funds from National Natural Science
673 Foundation of China (41772187, 42130307). P. Wu is grateful to the support from the
674 China Scholarship Council.

675

676 **Figure captions**

677 **Fig. 1.** Simplified geological map of South China (A), and the northern margin of the
678 Yangtze craton (B) and highlighting the distribution of Neoproterozoic and older
679 rocks units (adapted from [Zhao et al., 2022](#)).

680

681 **Fig. 2.** Distribution of Neoproterozoic igneous rocks in the northern margin of the
682 Yangtze craton with reliable zircon U-Pb ages labelled. Insets illustrate schematic
683 tectonics evolution of different stages.

684

685 **Fig. 3.** Histograms of the zircon U-Pb ages of Neoproterozoic igneous rocks (A-E)
686 from different domes of the northern margin of the South China Block. Detrital zircon
687 U-Pb ages of sedimentary rocks from the Bikou, South Qinling and Dahongshan areas
688 are also shown for comparison. See “[Supplementary](#) Table S1 and S5” for references.

689

690 **Fig. 4.** (A-D) U-Pb age versus zircon $\varepsilon_{\text{Hf}}(t)$, and (E-H) U-Pb age versus zircon O for
691 the igneous rocks from the northern Yangtze. Mantle zircon O values of $5.3 \pm 0.6\%$
692 (2s, [Valley et al., 1998](#)). In [Supplementary](#) Table S3-4 for references.

693

694 **Fig. 5.** Chemical classification diagrams of $\text{Na}_2\text{O} + \text{K}_2\text{O}$ versus SiO_2 (Middlemost,
695 Rickwood, 1989) and AFM diagram (Irvine and Baragar,
696 1971). The classification boundary of AFM diagrams are from Kuno (1968). For
697 references of compiled data, please see “[Supplementary Table S2](#)”.

698

699 **Fig. 6.** Primitive-mantle-normalized trace element patterns of Neoproterozoic rocks
700 from the northern Yangtze Block. Data for normalization are from McDonough and
701 Sun (1995). The compositions of OIB, E-MORB and N-MORB for comparison are
702 from Sun and McDonough (1989). The composition of average Andean and Aleutian
703 arc basalts are from Kelemen et al. (2003). In [Supplementary Table S2](#) for references.
704

705

705 **Fig. 7.** Time–space plot for various fragments of the northern margin of the South
706 China Block for the period from the end of the Mesoproterozoic to the early Paleozoic.
707 Sources of data for individual columns given in [Supplementary Table S1](#).
708

709

709 **Fig. 8.** Schematic reconstructions place South China at high latitudes connected to
710 India at the periphery of Rodinia, which satisfies the ca. 755 and 780 Ma
711 paleomagnetic data and allows for an active margin along the northern to western
712 margin of South China at this time. Modified after Park et al. (2021).
713

714 **Reference**

- 715 Ames, L., Zhou, G., Xiong, B., 1996. Geochronology and isotopic character of
716 ultrahigh-pressure metamorphism with implications for collision of the Sino-
717 Korean and Yangtze cratons, central China, *Tectonics*, 15, 472–489.
718 <https://doi.org/10.1029/95TC02552>
- 719 Ao, W., Zhao, Y., Zhang, Y., Zhai, M., Zhang, H., Zhang, R., Wang, Q., Sun, Y., 2019.
720 The Neoproterozoic magmatism in the northern margin of the Yangtze Block:
721 Insights from Neoproterozoic (950–706 Ma) gabbroic-granitoid rocks of the
722 Hannan Complex. *Precambrian Res.* 333, 105442.
723 <https://doi.org/10.1016/j.precamres.2019.105442>
- 724 Bader, T., Ratschbacher, L., Franz, L., Yang, Z., Hofmann, M., Linnemann, U., Yuan,
725 H., 2013. The heart of China revisited, I. Proterozoic tectonics of the Qin

- 726 mountains in the core of supercontinent Rodinia. *Tectonics* 32, 661–687.
727 <https://doi.org/10.1002/tect.20024>
- 728 Bai, Z.A., Shi, Y., Liu, X.J., Huang, Q.W., Qin, K.L., 2019. Geochronology,
729 Geochemistry and Hf Isotopes of Fengzishan Pluton in South Qinling and Its
730 Geological Significance. *Earth Science* 44, 1186–1201 (in Chinese with English
731 abstract). <https://doi.org/10.3799/dqkx.2018.586>
- 732 Barovich, K.M., Foden, J., 2000. A Neoproterozoic flood basalt province in southern-
733 central Australia: geochemical and Nd isotope evidence from basin fill.
734 *Precambrian Res.* 100, 213–234. [https://doi.org/10.1016/S0301-9268\(99\)00075-3](https://doi.org/10.1016/S0301-9268(99)00075-3)
- 735 Berkana, W., Wu, H., Ling, W., Kusky, T., Ding, X., 2022. Neoproterozoic
736 metavolcanic suites in the Micangshan terrane and their implications for the
737 tectonic evolution of the NW Yangtze block, South China. *Precambrian Research*
738 368, 106476. <https://doi.org/10.1016/j.precamres.2021.106476>
- 740 Bindeman, I.N., Simakin, A.G. 2014. Rhyolites—Hard to produce, but easy to recycle
741 and sequester: Integrating microgeochemical observations and numerical models.
742 *Geosphere* 10, 930–957. <https://doi.org/10.1130/GES00969.1>
- 743 Bindeman, I.N., Valley, J.W., 2001. Low- $\delta^{18}\text{O}$ rhyolites from Yellowstone: Magmatic
744 evolution based on analyses of zircons and individual phenocrysts. *Journal of
745 Petrology*, 42, 1491–1517. <https://doi.org/10.1093/petrology/42.8.1491>
- 746 Cai, W.C., Zeng, Z.C., Zhao P., Yang Z., Li J., Wang M., Zhu X., Zhang X., 2021. The
747 discovery of Neoproterozoic adakitic rocks in the east of South Qinling and its
748 geological significance. *Acta Geologica Sinica* 95, 686–702 (in Chinese with
749 English abstract). <https://doi.org/10.19762/j.cnki.dizhixuebao.2021117>
- 750 Cai, Z.Y., Xiong, X.L., Luo, H., Wu, D.K., Sun, S.C., Rao, B.L., Wang, S.X., 2007.
751 Forming age of the volcanic rocks of the Yaolinghe Group from Wudang Block,
752 Southern Qinling Mountain: constraint from Grain-Zircon U–Pb dating. *Acta
753 Geologica Sinica* 81, 620–625 (in Chinese with English abstract).
- 754 Cawood, P.A., Wang, Y.J., Xu, Y.J., Zhao, G.C., 2013. Locating south China in
755 Rodinia and Gondwana: A fragment of greater India lithosphere? *Geology*, 41,
756 903–906. <https://doi.org/10.1130/G34395.1>
- 757 Cawood, P.A., Zhao, G., Yao, J., Wang, W., Xu, Y., Wang, Y., 2018. Reconstructing
758 south China in Phanerozoic and Precambrian supercontinents. *Earth Sci. Rev.*
759 186, 173–194. <https://doi.org/10.1016/j.earscirev.2017.06.001>
- 760 Chang, L., Zhang, S., Li, H., Xian, H., Wu, H., Yang, T., 2022. New paleomagnetic
761 insights into the Neoproterozoic connection between South China and India and
762 their position in Rodinia. *Geophysical Research Letters*, 49, e2022GL098348.
763 <https://doi.org/10.1029/2022GL098348>
- 764 Chen, Y., K. Ye, J. B. Liu, and M. Sun., 2006a. Multistage metamorphism of the
765 Huangtuling granulite, Northern Dabie Orogen, eastern China: Implications for
766 the tectonometamorphic evolution of subducted lower continental crust, *J.
767 Metamorphic Geol.*, 24, 633–654. <https://doi.org/10.1111/j.1525-1314.2006.00659.x>
- 769 Chen, Z.H., Lu, S.N., Li, H.K., Li, H.M., Xiang, Z.Q., Zhou, H.Y., Song, B., 2006b.

- 770 Constraining the role of the Qinling orogen in the assembly and break-up of
771 Rodinia: tectonic implications for Neoproterozoic granite occurrences. *Journal of*
772 *Asian Earth Sciences* 28, 99–115. <https://doi.org/10.1016/j.jseaes.2005.03.011>
- 773 Collins, W.J., Richards, S.W., 2008. Geodynamic significance of S-type granites in
774 circum-Pacific orogens. *Geology* 36, 559–562.
775 <https://doi.org/10.1130/G24658A.1>
- 776 Corti, G., 2009. Continental rift evolution: From rift initiation to incipient break-up in
777 the Main Ethiopian Rift, East Africa. *Earth-Science Reviews* 96, 1–53.
778 <https://doi.org/10.1016/j.earscirev.2009.06.005>
- 779 Cui, J., Wang F., Duan, J., Zhao, S., Cui, H., Cui, H., 2013. The Sunjiahe Formation
780 of the Xixiang Group, southern Qinling Ranges: SHRIMP zircon U-Pb age and
781 its tectonic implications. *Sedimentary Geology and Tethyan Geology* 33, 1–5 (in
782 Chinese with English abstract).
- 783 Cui, J.T., Han, F.L., Zhang, S.H., Wang, G.B., Wang, B.Y., Wang, X.P., Peng, H.L.,
784 Wang, J. A., Guo, Q.M., Peng, A.Y., Dui, H.M., 2010. Zircon SHRIMP U-Pb
785 dating and the tectonic significance of the Xixiang Group in southern Qinling.
786 *Geol. Shanxi* 2, 53–58 (in Chinese with English Abstract).
- 787 DeCelles, P.G., Ducea, M.N., Kapp, P., Zandt, G., 2009. Cyclicity in Cordilleran
788 orogenic systems. *Nat. Geosci.* 2, 251–257. <https://doi.org/10.1038/ngeo469>
- 789 Deng, H., Peng, S.B., Polat, A., Kusky, T., Jiang, X.F., Han, Q.S., Wang, L., Huang, Y.,
790 Wang, J.P., Zeng, W., Hu, Z.X., 2017. Neoproterozoic IAT intrusion into
791 Mesoproterozoic MOR Miaowan Ophiolite, Yangtze Craton: Evidence for
792 evolving tectonic settings. *Precambr. Res.* 289, 75–94.
793 <https://doi.org/10.1016/j.precamres.2016.12.003>
- 794 Deng, Q., Wang, J., Wang, Z.J., Jiang, X.S., Du, Q.D., Wu, H., Yang, F., Cui, X.Z.,
795 2013a. Zircon U-Pb ages for tuffs from the Dashigou and Sanlangpu Formations
796 of the Xixiang Group in the northern margin of Yangtze Block and their
797 geological significance. *J. Jilin Univ. (Earth Sci. Ed.)* 3, 797–808 (in Chinese
798 with English Abstract). <http://xuebao.jlu.edu.cn/dxb/EN/Y2013/V43/I3/797>
- 799 Deng, Q., Wang, J., Wang, Z.J., Wang, X.C., Qiu, Y.S., Yang, Q.X., Du, Q.D., Cui,
800 X.Z., Zhou, X.L., 2013b. Continental flood basalts of the Huashan Group,
801 northern margin of the Yangtze block – implications for the breakup of Rodinia.
802 *Int. Geol. Rev.* 55, 1865–1884. <https://doi.org/10.1080/00206814.2013.799257>
- 803 Deng, Q., Wang, Z., Ren, G., et al., 2020. Identification of the ~2.09Ga and ~1.76 Ga
804 granitoids in the northwestern Yangtze Block: Records of the assembly and
805 break-up of Columbia supercontinent. *Earth Science* 45, 3295–3312.
806 <https://doi.org/10.3799/dqkx.2020.182>
- 807 Deng, Q., Wang, Z., Wang, J., Cui, X., Ma, L., Xiong, X., 2017. Discovery of the
808 Baiyu ~1.79 Ga A-type granite in the Beiba area of the northwestern margin of
809 Yangtze Block: Constraints on tectonic evolution of South China. *Acta*
810 *Geologica Sinica* 91, 1454–1466 (in Chinese with English abstract).
- 811 Deng, Q.Z., Yang, Q.X., Mao, X.W., Kong, L.Y., 2016. Study of Lithostratigraphic
812 Sequences and Chronology of Middle-late Nanhua in Wudang-Suizhou Area.
813 *Resources Environment & Engineering* 30, 132–142 (in Chinese with English

- 814 abstract).
- 815 Dong, Y.P., Liu, X.M., Santosh, M., Chen, Q., Zhang, X.N., Li, W., He, D.F., Zhang,
816 G.W., 2012. Neoproterozoic accretionary tectonics along the northwestern
817 margin of the Yangtze Block, China: constraints from zircon U-Pb
818 geochronology and geochemistry. *Precambr. Res.* 196–197, 247–274.
819 <https://doi.org/10.1016/j.precamres.2011.12.007>
- 820 Dong, Y.P., Liu, X.M., Santosh, M., Zhang, X.N., Chen, Q., Yang, C., Yang, Z., 2011a.
821 Neoproterozoic subduction tectonics of the northwestern Yangtze Block in South
822 China: constrains from zircon U-Pb geochronology and geochemistry of mafic
823 intrusions in the Hannan Massif. *Precambr. Res.* 189, 66–90.
824 <https://doi.org/10.1016/j.precamres.2011.05.002>
- 825 Dong, Y., Zhang, G., Neubauer, F., Liu, X., Genser, J., Hauzenberger C., 2011b.
826 Tectonic evolution of the Qinling orogen, China: Review and synthesis, *J Asian
827 Earth Sci.*, 41, 213–237. <https://doi.org/10.1016/j.jseaes.2011.03.002>
- 828 Dong, Y.P., Sun, S.S., Yang, Z., Liu, X.M., Zhang, F.F., Li, W., Cheng, B., He, D.F.,
829 Zhang, G.W., 2017. Neoproterozoic subduction-accretionary tectonics of the
830 South Qinling Belt, China. *Precambrian Research* 293, 73–90.
831 <https://doi.org/10.1016/j.precamres.2017.02.015>
- 832 Druschke, P., Hanson, A.D., Yan, Q., Wang, Z., Wang, T., 2006. Stratigraphic and U-
833 Pb SHRIMP detrital zircon evidence for a Neoproterozoic continental arc,
834 Central China: Rodinia implications, *J. Geol.*, 114, 627–636.
835 <https://doi.org/10.1086/506162>
- 836 Duan, B., Su, L., Wang, J., Xiao, L., 2018. Origin of Neoproterozoic complexes in the
837 northwestern margin of the Yangtze plate Sangxigou granite: Breakup of the
838 Rodinia supercontinent and melting of the crust. *Geochimica* 47, 506–521 (in
839 Chinese with English abstract).
- 840 Duan, S.S., Jiao, J.G., Luo, D.Z., Huang, X.F., Wang, S., Chen, B.L., 2017. Zircon U-
841 Pb Geochronology of Intermediate-Felsic Dykes from the Jiangjunhe area in
842 northern Shiquan, South Qinling Mountains and its geological Significance. *Acta
843 Geologica Sinica* 91, 748–761 (in Chinese with English abstract).
- 844 Du, Q., Wang, Z., Wang, J., Deng, Q., Yang, F., 2016. Geochronology and
845 geochemistry of tuff beds from the Shicaohe Formation of Shennongjia Group
846 and tectonic evolution in the northern Yangtze Block, South China. *Int J Earth
847 Sci (Geol Rundsch)* 105, 521–535. <https://doi.org/10.1007/s00531-015-1182-2>
- 848 Evans, D.A.D., 2009, The palaeomagnetically viable, long-lived and all-inclusive
849 Rodinia supercontinent reconstruction, in Murphy, J.B., et al., eds., *Ancient
850 orogens and modern analogues: Geological Society of London Special
851 Publication* 327, 371–404. <https://doi.org/10.1144/SP327.16>
- 852 Fu, B., Kita, N.T., Wilde, S.A., Liu, X., Cliff, J., Greig, A., 2013. Origin of the
853 Tongbai-Dabie-Sulu Neoproterozoic low- $\delta^{18}\text{O}$ igneous province, east-central
854 China. *Contrib. Mineral. Petrol.* 165, 641–662. <https://doi.org/10.1007/s00410-012-0828-3>
- 856 Fu, H., Zhang, S., Condon, D., Xian, H., 2022. Secular change of true polar wander
857 over the past billion years. *Sci. Adv.*, 8 (41), eabo2753.

- 858 <https://doi.org/10.1126/sciadv.abo2753>
- 859 Gan, B.P., Lai, S.C., Qin, J.F., Zhu, R.Z., Zhao, S.W., Li, T., 2017. Neoproterozoic
860 alkaline intrusive complex in the northwestern Yangtze Block, Micang
861 Mountains region, South China: petrogenesis and tectonic significance. Int. Geol.
862 Rev. 59, 311–332. <https://doi.org/10.1080/00206814.2016.1258676>
- 863 Gao, F., Pei, X.Z., Li, R.B., Li, Z.C., Pei, L., Chen, Y.X., Wang, M., Zhao, S.W., Liu,
864 C.J., Li, X.B., 2020. Neoproterozoic tectonic evolution of the northwestern
865 margin of the Yangtze Block (southwestern China): Evidence from sandstone
866 geochemistry and detrital zircon U-Pb ages of the Hengdan Group. Precambr.
867 Res. 344, 105737. <https://doi.org/10.1016/j.precamres.2020.105737>
- 868 Geng, Y.-Y., 2010. SHRIMP U-Pb zircon geochronology and geochemistry study of
869 Neoproterozoic granites in the northern margin of Yangtze continent.
870 Dissertation Submitted to China. University of Geosciences for Master Degree,
871 pp. 1-60 (In Chinese).
- 872 Greentree, M.R., Li, Z.-X., Li, X.-H., Wu, H., 2006. Late Mesoproterozoic to earliest
873 Neoproterozoic basin record of the Sibao orogenesis in western South China and
874 relationship to the assembly of Rodinia. Precambrian Res. 151, 79-100.
875 <https://doi.org/10.1016/j.precamres.2006.08.002>
- 876 Guo, X.Q., Yan, Z., Wang, Z.Q., Fu, C.L., Chen, L., 2014. Tectonic setting of
877 Lijiabian Ti-Fe deposit in Shanyang-Zhashui ore concentration area, Qinling
878 Orogen. Acta Petrologica Sinica 30, 437-450 (in Chinese with English abstract).
- 879 He, Q., Zhang, S.B., Zheng, Y.F., 2016. High temperature glacial meltwater–rock
880 reaction in the Neoproterozoic: Evidence from zircon in-situ oxygen isotopes in
881 granitic gneiss from the Sulu orogen. Precambrian Res. 284, 1-13.
882 <https://doi.org/10.1016/j.precamres.2016.07.012>
- 883 He, Q., Zhang, S.B., Zheng, Y.F., 2018. Evidence for regional metamorphism in a
884 continental rift during the Rodinia breakup. Precambrian Res. 314, 414-427.
885 <https://doi.org/10.1016/j.precamres.2018.06.009>
- 886 He, Y., Wu, Y-B., Zhao, Y., Zhou, G-Y., 2020. Neoproterozoic Amphibolite-Facies
887 Metamorphism of Douling Complex at the Northern Margin of the Yangtze
888 Craton. <http://doi.org/10.46427/gold2020.1003>
- 889 HGB (Hubei Geological Bureau), 1982. 1:200,000 Regional Geological Investigation
890 Report for the Suixian Area, Hubei Province, the People's Republic of China,
891 294pp (in Chinese).
- 892 Hofmann, M., Linnemann, U., Rai, V., Becker, S., Gärtner, A., Sagawe, A., 2011. The
893 India and South China cratons at the margin of Rodinia-Synchronous
894 Neoproterozoic magmatism revealed by LA-ICP-MS zircon analyses. Lithos 123,
895 176–187. <https://doi.org/10.1016/j.lithos.2011.01.012>
- 896 Hu, F., Liu, S., Santosh, M., Deng, Z., Wang, W., Zhang, W., Yan, M., 2016.
897 Chronology and tectonic implications of Neoproterozoic blocks in the South
898 Qinling Orogenic Belt, Central China. Gondwana Research 30, 24-47.
899 <https://doi.org/10.1016/j.gr.2015.01.006>
- 900 Hu, J., G. Zhao, Q. Meng, H. Luo, and Z. Wang., 2002. The geological features and
901 tectonic significances of the basic swarms in Wudang terrain of Qinling orogen.

- 902 Acta Petrol Sinica, 19, 601-611.
- 903 Hu, J., Liu, X., Chen, L., Qu, W., Li, H., Geng, J., 2013. A ~2.5 Ga magmatic event at
904 the northern margin of the Yangtze craton: Evidence from U-Pb dating and Hf
905 isotope analysis of zircons from the Douling Complex in the South Qinling
906 orogen. Chinese Science Bulletin 58, 3564-3579. <https://doi.org/10.1007/s11434-013-5904-1>
- 907 Hu, J., Liu, X.C., Qu, W., Chen, L.Y., 2019. Mid-Neoproterozoic amphibolite facies
908 metamorphism at the northern margin of the Yangtze craton. Precambrian
909 Research 326, 333-343. <https://doi.org/10.1016/j.precamres.2017.10.010>
- 910 Hu, Z.X., Chen, C., Mao, X.W., Deng, Q.Z., Yang, J.X., Li, L.L., Kong, L.Y., 2015.
911 Documentation of Jingningian Island-arc Volcanic Rocks and Accretionary
912 Complexes in the Dahongshan Region, Northern Hubei and Its Tectonic
913 Significance. Resources Environment & Engineering 29, 757-766 (in Chinese
914 with English abstract).
- 915 Huang, H.Y., He, D.F., Li, D., Li, Y.Q., 2021a. Zircon U-Pb ages and Hf isotope
916 analysis of Neoproterozoic Yaolinghe Group sedimentary rocks in the Chengkou
917 area, South Qinling: Provenance and paleogeographic implications. Precambrian
918 Research 355, 106088. <https://doi.org/10.1016/j.precamres.2020.106088>
- 919 Huang, Y., Wang, X.L., Li, J.Y., Wang, D., Jiang, C.H., Li, L.S., 2021b. Early
920 Neoproterozoic tectonic evolution of northern Yangtze Block: Insights from
921 sedimentary sequences from the Dahongshan area. Precambrian Res. 365,
922 106382. <https://doi.org/10.1016/j.precamres.2021.106382>
- 923 Huang, Y., Wang, X., Li, J.Y., et al., 2023. From arc accretion to within-plate
924 extension: Geochronology and geochemistry of the Neoproterozoic magmatism
925 on the northern margin of the Yangtze Block. Precambrian Res. 395, 107133.
926 <https://doi.org/10.1016/j.precamres.2023.107133>
- 927 Hubei, R.G.S., 1990. Regional Geology of Hubei Province (in Chinese). Geological
928 Publishing House, Beijing.
- 929 Hui, B., 2021. Neoproterozoic tectonic evolution of the Bikou Terrane, northwestern
930 margin of the Yangtze Block. Dissertation Submitted to China. Northwest
931 University for Ph. Degree, pp. 143–166 (in Chinese).
- 932 Hui, B., Dong, Y.P., Cheng, C., Long, X.P., Liu, X.M., Yang, Z., Sun, S.S., Zhang, F.F.,
933 Varga, J., 2017. Zircon U–Pb chronology, Hf isotope analysis and whole-rock
934 geochemistry for the Neoarchean-Paleoproterozoic Yudongzi complex,
935 northwestern margin of the Yangtze craton, China. Precambrian Research, 301,
936 65–8. <https://doi.org/10.1016/j.precamres.2017.09.003>
- 937 Hui, B., Dong, Y.P., Liu, G., Zhao, H., Sun, S.S., Zhang, F.F., Liu, X.M., 2020a.
938 Origin of mafic intrusions in the Micangshan Massif, Central China:
939 Implications for the Neoproterozoic tectonic evolution of the northwestern
940 Yangtze Block. J. Asian Earth Sci. 190, 104132.
941 <https://doi.org/10.1016/j.jseae.2019.104132>
- 942 Hui, B., Dong, Y.P., Zhang, F.F., Sun, S.S., He, S., 2020b. Neoproterozoic active
943 margin in the northwestern Yangtze Block, South China: New clues from detrital
944 zircon U-Pb geochronology and geochemistry of sedimentary rocks from the
945

- 946 Hengdan Group. Geol. Mag. <https://doi.org/10.1017/S0016756820000898>
- 947 Hui, B., Dong, Y.P., Zhang, F.F., Sun, S.S., He, S., 2021. Petrogenesis and tectonic
948 implications of the Neoproterozoic mafic intrusions in the Bikou Terrane along
949 the northwestern margin of the Yangtze Block, South China. Ore Geology
950 Reviews, 2021, 131: 104014. <https://doi.org/10.1016/j.oregeorev.2021.104014>
- 951 Irvine, T.N., Baragar, W.R.A., 1971. A guide to the chemical classification of the
952 common volcanic rocks: Can. J. Earth Sci. 8, 523–548.
<https://doi.org/10.1139/e71-055>
- 953 Jing, X., Yang, Z., Tong, Y., Han, Z., 2015. A revised paleomagnetic pole from the
954 mid-Neoproterozoic Liantuo Formation in the Yangtze block and its
955 paleogeographic implications. Precambrian Res. 268, 194–211.
<https://doi.org/10.1016/j.precamres.2015.07.007>
- 956 Jing, X., Yang, Z., Evans, D.A.D., Tong, Y., Xu, Y., Wang, H., 2019. A pan-latitudinal
957 Rodinia in the Tonian true polar wander frame. Earth Planet. Sci. Lett. 530,
958 115880. <https://doi.org/10.1016/j.epsl.2019.115880>
- 959 Jing, X., Evans, D.A.D., Yang, Z., Tong, Y., Xu, Y., Wang, H., 2021. Inverted south
960 China A novel configuration for Rodinia and its breakup. Geology 49, 463–467.
<https://doi.org/10.1130/G47807.1>
- 961 Kelemen, P.B., Hanghøj, K., Greene, A.R., 2003. One View of the Geochemistry of
962 Subduction-related Magmatic Arcs, with an Emphasis on Primitive Andesite and
963 Lower Crust. Treatise Geochem. 3, 593–659. <https://doi.org/10.1016/B0-08-043751-6/03035-8>
- 964 Kemp, A.I.S., Hawkesworth, C.J., Collins, W.J., Gray, C.M., Blevin, P.L., 2009.
965 Isotopic evidence for rapid continental growth in an extensional accretionary
966 orogen: the Tasmanides, eastern Australia. Earth Planet. Sci. Lett. 284, 455–466.
<https://doi.org/10.1016/j.epsl.2009.05.011>
- 967 Kuno, H., 1968. Differentiation of basalt magmas. In: Hess, H.H., Poldervaart,
968 A.(Eds.), Basalts: The Poldervaart Treatise on Rocks of Basaltic Composition.
969 Wiley-Interscience, New York, pp. 623–688.
- 970 Lai, S.C., Li, Y.F., Qin, J.F., 2007. Geochemistry and LA-ICP-MS zircon U–Pb dating
971 of the Dongjiahe ophiolite complex from the western Bikou terrane. Science in
972 China (Series D) 50 (Suppl. II), 305–313. <https://doi.org/10.1007/s11430-007-6006-1>
- 973 Lan, Z., Li, X.-H., Zhang, Q., Li, Q.-L., 2015a. Global synchronous initiation of the
974 2nd episode of Sturtian glaciation: SIMS zircon U–Pb and O isotope evidence
975 from the Jiangkou group, south China. Precambrian Research, 267, 28–38.
<https://doi.org/10.1016/j.precamres.2015.06.002>
- 976 Lan, Z., Li, X.-H., Zhu, M., Zhang, Q., Li, Q.-L., 2015b. Revisiting the Liantuo
977 Formation in Yangtze block, south China: SIMS U–Pb zircon age constraints and
978 regional and global significance. Precambrian Research, 263, 123–141.
<https://doi.org/10.1016/j.precamres.2015.03.012>
- 979 Lan, Z., Huyskens, M.H., Le Hir, G., Mitchell, R.N., Yin, Q.-Z., Zhang, G., Li, X.-H.,
980 2022. Massive volcanism may have foreshortened the Marinoan snowball Earth.
981 Geophysical Research Letters, 49, e2021GL097156.

- 990 <https://doi.org/10.1029/2021GL097156>
- 991 Lawton, T.F., McMillan, N.J., 1999. Arc abandonment as a cause for passive
992 continental rifting: Comparison of the Jurassic Mexican Borderland rift and the
993 Cenozoic Rio Grande rift. *Geology*, 27, 779–782. [https://doi.org/10.1130/0091-7613\(1999\)027<0779:AAAACF>2.3.CO;2](https://doi.org/10.1130/0091-7613(1999)027<0779:AAAACF>2.3.CO;2)
- 994 Li, H.K., Lu, S.N., Chen, Z.H., Xia, Z.Q., Zhou, H.Y., Hao, G.J., 2003a. Zircon U-Pb
995 geochronology of rift-type volcanic rocks of the Yaolinghe Group in the South
996 Qinling orogen. *Geological Bulletin of China* 22, 775-781 (in Chinese with
997 English abstract).
- 998 Li, H.K., Zhang, C.L., Xiang, Z.Q., Lu, S.N., Zhang, J., Geng, J.Z., Qu, L.S., Wang,
999 Z.X., 2013. Zircon and baddeleyite U-Pb geochronology of the Shennongjia
1000 Group in the Yangtze Craton and its tectonic significance. *Acta Petrol. Sin.* 29,
1001 673–697 (in Chinese with English Abstract).
- 1002 Li, J., Zhu, S., 1930. Geological study in mid-south Qingling. *Coll. Paper. Inst. Geol.*
1003 *Res., Chin. Centr. Res. Inst.*, 1930 (A19): 1-103 (in Chinese).
- 1004 Li, J.H., Zhang, Y.Q., Xu, X.B., Dong, S.W., Li, T.D., 2012. Zircon U-Pb LA-ICP-MS
1005 dating of Fenghuangshan pluton in Northern Daba mountains and its
1006 implications to tectonic settings. *Geological Review* 58, 581-593 (in Chinese
1007 with English abstract).
- 1008 Li, J.Y., Wang, X.L., Gu, Z.D., 2018a. Early Neoproterozoic arc magmatism of the
1009 Tongmuliang Group on the northwestern margin of the Yangtze Block:
1010 Implications for Rodinia assembly. *Precambrian Res.* 309, 181–197.
1011 <https://doi.org/10.1016/j.precamres.2017.04.040>
- 1012 Li, J.Y., Wang, X.L., Gu, Z.D., 2018b. Petrogenesis of the Jiaoziding granitoids and
1013 associated basaltic porphyries: Implications for extensive early Neoproterozoic
1014 arc magmatism in western Yangtze Block. *Lithos*, 296-299, 547-562.
1015 <https://doi.org/10.1016/j.lithos.2017.11.034>
- 1016 Li, J.Y., Wang, X.L., Wang, D., Du, D.H., Yu, J.H., Gu, Z.D., Huang, Y., Li, L.S.,
1017 2021a. Pre-Neoproterozoic continental growth of the Yangtze Block: From
1018 continental rifting to subduction–accretion. *Precambrian Res.* 355, 106081.
1019 <https://doi.org/10.1016/j.precamres.2020.106081>
- 1020 Li, J.Y., Tang, M., Lee, C.T., Wang, X.L., Gu, Z.D., Xia, X.P., Wang, D., Du, D.H., Li,
1021 L.S., 2021b. Rapid endogenic rock recycling in magmatic arcs. *Nature*
1022 *Communication*, 12, 3533. <https://doi.org/10.1038/s41467-021-23797-3>
- 1023 Li, K., Deng, Q., Hou, M., Wang, J., Yakymchuk, C., Cui, X., Ren, G., Wang, Z., 2020.
1024 Geochronology and sedimentology of the Huashan Group in the northern
1025 Yangtze Block: implications for the initial breakup of the South China. *Int. J.*
1026 *Earth Sci.* 109, 2113–2131. <https://doi.org/10.1007/s00531-020-01890-0>
- 1027 Li, L.M., Lin, S.F., Xing, G.F., Davis, D.W., Davis, W.J., Xiao, W.J., Yin, C.Q., 2013b.
1028 Geochemistry and tectonic implications of late Mesoproterozoic alkaline
1029 bimodal volcanic rocks from the Tieshajie Group in the southeastern Yangtze
1030 Block, South China. *Precambrian Res.* 230, 179–192.
1031 <https://doi.org/10.1016/j.precamres.2013.02.004>
- 1032 Li, Q.W., Zhao, J.H., 2016. Petrogenesis of the Wudang mafic dikes: Implications of
1033

- 1034 changing tectonic settings in South China during the Neoproterozoic.
1035 Precambrian Res. 272, 101–114. <https://doi.org/10.1016/j.precamres.2015.10.019>
- 1036 Li, X.H., Li, Z.X., Zhou, H., Liu, Y., Kinny, P.D., 2002. U–Pb zircon geochronology,
1037 geochemistry and Nd isotopic study of Neoproterozoic bimodal volcanic rocks in
1038 the Kangdian Rift of South China: implications for the initial rifting of Rodinia.
1039 Precambrian Res. 113, 135–154. [https://doi.org/10.1016/S0301-9268\(01\)00207-8](https://doi.org/10.1016/S0301-9268(01)00207-8)
- 1040 Li, X.H., Li, Z.X., Zhou, H.W., Liu, Y., Liang, X.R., Li, W.X., 2003b. SHRIMP U–Pb
1041 zircon age, geochemistry and Nd isotope of the Guandaoshan pluton in SW
1042 Sichuan: petrogenesis and tectonic significance. Sci. China Ser. D 46 (Suppl.),
1043 73–83. <https://doi.org/10.1360/03dz9029>
- 1044 Li, X.H., Li, Z.X., Ge, W.C., Zhou, H.W., Li, W.X., Liu, Y., Wingate, M.T.D., 2003c.
1045 Neoproterozoic granitoids in South China: crustal melting above a mantle plume
1046 at ca 825 Ma? Precambrian Research 122, 45–83. [https://doi.org/10.1016/S0301-9268\(02\)00207-3](https://doi.org/10.1016/S0301-9268(02)00207-3)
- 1047 Li, X.H., Li, Z.X., Sinclair, J.A., Li, W.X., Carter, G., 2007. Reply to the comment by
1048 Zhou et al. on: “Revisiting the “Yanbian Terrane”: Implications for
1049 Neoproterozoic tectonic evolution of the western Yangtze Block, South China”
1050 [Precambrian Res. 151 (2006) 14–30] [Precambrian Res. 154 (2007) 153–157].
1051 Precambrian Res. 155, 318–323. <https://doi.org/10.1016/j.precamres.2006.11.012>
- 1052 Li, X.-H., Li, W.-X., Li, Z.-X., Lo, C.-H., Wang, J., Ye, M.-F., Yang, Y.-H., 2009.
1053 Amalgamation between the Yangtze and Cathaysia Blocks in South China:
1054 constraints from SHRIMP U–Pb zircon ages, geochemistry and Nd–Hf isotopes
1055 of the Shuangxiwu volcanic rocks. Precambrian Res. 174, 117–128.
1056 <https://doi.org/10.1016/j.precamres.2009.07.004>
- 1057 Li, X.-H., Li, Z.-X., Li, W.-X., 2014. Detrital zircon U–Pb age and Hf isotope
1058 constrains on the generation and reworking of Precambrian continental crust in
1059 the Cathaysia Block, South China: a synthesis. Gondwana Res. 25, 1202–1215.
1060 <https://doi.org/10.1016/j.gr.2014.01.003>
- 1061 Li, Y., Wang, G., Wang, C., Chang, H., 2000. Zircon U–Pb isotopic geochronology of
1062 the Longcaoping crystal complex in Southern Qinling. Acta Mineral. Sinica, 20,
1063 50–54 (in Chinese with English abstract).
- 1064 Li, Z.X., Zhang, L.H., Powell, C.M., 1995. South China in Rodinia: part of the
1065 missing link between Australia-East Antarctica and Laurentia? Geology 23, 407–
1066 410. [https://doi.org/10.1130/0091-7613\(1995\)023<407:SCIRPO>2.3.CO;2](https://doi.org/10.1130/0091-7613(1995)023<407:SCIRPO>2.3.CO;2)
- 1067 Li, Z.X., Li, X.H., Zhou, H., Kinny, Peter D., 2002. Grenvillian continental collision
1068 in south China: New SHRIMP U–Pb zircon results and implications for the
1069 configuration of Rodinia. Geology, 30, 163–166. [https://doi.org/10.1130/0091-7613\(2002\)030<0163:GCCISC>2.0.CO;2](https://doi.org/10.1130/0091-7613(2002)030<0163:GCCISC>2.0.CO;2)
- 1070 Li, Z.X., Li, X.H., Kinny, P.D., Wang, J., Zhang, S., Zhou, H., 2003a. Geochronology
1071 of Neoproterozoic syn-rift magmatism in the Yangtze Craton, South China and
1072 correlations with other continents: evidence for a mantle superplume that broke
1073 up Rodinia. Precambrian Research 122, 85–109. [https://doi.org/10.1016/S0301-9268\(02\)00208-5](https://doi.org/10.1016/S0301-9268(02)00208-5)
- 1074 Li, Z.-X., Wartho, J.-A., Occhipinti, S., Zhang, C.-L., Li, X.-H., Wang, J., Bao, C.,
1075

- 1078 2007. Early history of the eastern Sibao Orogen (South China) during the
1079 assembly of Rodinia: New mica $^{40}\text{Ar}/^{39}\text{Ar}$ dating and SHRIMP U–Pb detrital
1080 zircon provenance constraints. *Precambrian Res.* 159, 79–94.
1081 <https://doi.org/10.1016/j.precamres.2007.05.003>
- 1082 Li, Z.X., Bogdanova, S.V., Collins, A.S., Davidson, A., De Waele, B., Ernst, R.E.,
1083 Fitzsimons, I.C.W., Fuck, R.A., Gladkochub, D.P., Jacobs, J., Karlstrom, K.E.,
1084 Lu, S., Natapov, L.M., Pease, V., Pisarevsky, S., Thrane, A.K., Vernikovsky, V.,
1085 2008. Assembly, configuration, and break-up history of Rodinia: a synthesis.
1086 *Precambr. Res.* 160, 179–210. <https://doi.org/10.1016/j.precamres.2007.04.021>
- 1087 Liao, M.F., Xie, Y.B., Li, L.J., Yang, J.X., Mao, X.W., Deng, Q.Z., Kong, L.Y., Li,
1088 Q.W., Chen, C., 2016. Discussion about Genesis and Formation Age of
1089 Sanligang Pluton in the Dahongshan Region, Hubei. *Resources Environment &*
1090 *Engineering* 30, 143–158 (in Chinese with English abstract).
- 1091 Ling, W., Gao, S., Ouyang, J., Zhang, B., Li, H., 2002. Time and tectonic setting of
1092 the Xixiang Group: Constraints from zircon U–Pb geochronology and
1093 geochemistry. *Science in China Series D: Earth Sciences* 45, 818–831.
1094 <https://doi.org/10.1007/BF02879516>
- 1095 Ling, W., Gao, S., Zhang, B., Li, H., Liu, Y., Cheng, J., 2003. Neoproterozoic tectonic
1096 evolution of the northwestern Yangtze craton, South China: implications for
1097 amalgamation and break-up of the Rodinia Supercontinent. *Precambrian Res.*
1098 122, 111–140. [https://doi.org/10.1016/S0301-9268\(02\)00222-X](https://doi.org/10.1016/S0301-9268(02)00222-X)
- 1099 Ling, W., Ren, B., Duan, R., Liu, X., Mao, X., Peng, L., Liu, Z., Cheng, J., Yang, H.,
1100 2008. Timing of the Wudangshan, Yaolinghe volcanic sequences and mafic sills
1101 in South Qinling: U–Pb zircon geochronology and tectonic implication. *Chinese*
1102 *Science Bulletin* 53, 2192–2199. <https://doi.org/10.1007/s11434-008-0269-6>
- 1103 Ling, W.L., Gao, S., Cheng, J.P., Jiang, L.S., Yuan, H.L., Hu, Z.C., 2006.
1104 Neoproterozoic magmatic events within the Yangtze continental interior and
1105 along its northern margin and their tectonic implication: constraint form the
1106 ELA-ICPMS U–Pb geochronology of zircons from the Huangling and Hannan
1107 complexes. *Acta Petrologica Sinica* 22, 387–396 (in Chinese with English
1108 abstract).
- 1109 Lister, G.S., Forster, M.A., Rawlings, T.J., 2001. Episodicity during orogenesis. In:
1110 MILLER, J. A., HOLDSWORTH, R. E., BUICK, I. S. & HAND, M. (eds)
1111 Continental Reactivaton and Reworking. Geological Society, London, Special
1112 Publications, 184, 89–113. <https://doi.org/10.1144/GSL.SP.2001.184.01.06>
- 1113 Liu C.H., Wu C.L., Gao Y.H., Lei M., Qin H.P., Li M.Z., 2014. Zircon LA-ICP-MS
1114 U–Pb dating and Lu-Hf isotopic system of Dongjiangkou, Zhashui, and
1115 Liyuantang granitoid intrusions, South Qinling belt, central China. *Acta*
1116 *Petrologica Sinica*, 30, 2402–2420. (in Chinese with English abstract).
- 1117 Liu, H., Zhao, J., Li, L., 2022. Opening of the Proto-Tethys Ocean: Implications from
1118 the late Neoproterozoic mafic dike swarms in the South Qinling Belt, South Chin.
1119 *Gondwana Research*, 101, 44–58. <https://doi.org/10.1016/j.gr.2021.06.023>
- 1120 Liu, H., Zhao, J.H., 2019. Slab breakoff beneath the northern Yangtze Block:
1121 Implications from the Neoproterozoic Dahongshan mafic intrusions. *Lithos* 342–

- 1122 343, 263–275. <https://doi.org/10.1016/j.lithos.2019.05.037>
- 1123 Liu, J., Zhang, L., 2013. Neoproterozoic low to negative $\delta^{18}\text{O}$ volcanic and intrusive
1124 rocks in the Qinling Mountains and their geological significance. Precambrian
1125 Res. 230, 138–167. <https://doi.org/10.1016/j.precamres.2013.02.006>
- 1126 Liu, J.W., Zhang, H.F., 2018. The petrogenesis and tectonic setting of the
1127 Neoproterozoic basic intrusions in the South Qinling orogenic belt: Constraints
1128 from the U-Pb geochronology and Hf-O isotopes. Journal of Northwest
1129 University (Natural Science Edition) 48, 268–283 (in Chinese with English
1130 abstract).
- 1131 Liu, R., Zhang, B.R., Zhang, H.F., Yuan, H.L., 2009. U-Pb zircon age, geochemical
1132 and Sr-Nd-Hf isotopic compositions of Neoproterozoic granitoids in
1133 northwestern margin of Yangtze block (South China): implications for
1134 Neoproterozoic tectonic evolution. J. Earth Sci. 20, 659–680.
1135 <https://doi.org/10.1007/s12583-009-0058-4>
- 1136 Liu, R.Y., Li, Q.S., Niu, B.G., He, Z.J., Ren, J.S., 2018. Geochemical Characteristics
1137 and Tectonic Implications of the Xiaomaoling Composite Intrusives in South
1138 Qinling Orogenic Belt. Acta Geoscientica Sinica 39, 201–215.
1139 <https://doi.org/10.3975/cagsb.2018.012501>
- 1140 Liu, R.Y., Niu, B.G., He, Z.J., Ren, J.S., 2011. LA-ICP-MS zircon U-Pb
1141 geochronology of the eastern part of the Xiaomaoling composite intrusives in
1142 Zhashui area, Shaanxi, China. Geological Bulletin of China 30, 448–460 (in
1143 Chinese with English abstract).
- 1144 Liu, R.Y., Niu, B.G., Li, C., 2020. Zircon SHRIMP U-Pb dating of the Wudang Group
1145 in South Qinling belt and its geological significance. Acta Petrologica et
1146 Mineralogica 39, 751–768 (in Chinese with English abstract).
- 1147 Liu, S.D., Zeng, Z.X., Guo, R.L., Zhang, X., 2021. Huashan Group in northern
1148 margin of Yangtze block: a suite of backarc-basin volcanic-sedimentary strata
1149 but not ophiolite mélange. Earth Science, 46, 2751–2767.
1150 <https://doi.org/10.3799/dqkx.2020.266>
- 1151 Lu, K., Li, X.H., Zhou, J.L., Peng, S.B., Deng, H., Guo, S., Yang, C., Wu, L.G., 2020.
1152 Early Neoproterozoic assembly of the Yangtze Block decoded from
1153 metasedimentary rocks of the Miaowan Complex. Precambrian Res. 346, 105787.
1154 <https://doi.org/10.1016/j.precamres.2020.105787>
- 1155 Lu, K., Mitchell, R.N., Yang, C., Zhou, J.L., Wu, L.G., Wang, X.C., Li, X.H., 2022.
1156 Widespread magmatic provinces at the onset of the Sturtian snowball Earth,
1157 Earth and Planetary Science Letters, 594, 117736.
1158 <https://doi.org/10.1016/j.epsl.2022.117736>
- 1159 Lu, X.X., Dong, Y., Wei, X.D., Xiao, Q.H., Li, X.P., Zhang, Z.Q., 1999. Age of
1160 Tuwushan A-type granite in east Qinling and its tectonic implications. Chinese
1161 Science Bulletin 44, 975–978 (in Chinese with English abstract).
- 1162 Luo, B.J., Liu, R., Zhang, H.F., Zhao, J.H., Yang, H., Xu, W.C., Guo, L., Zhang, L.Q.,
1163 Tao, L., Pan, F.B., Wang, W., Gao, Z., Shao, H., 2018. Neoproterozoic
1164 continental back-arc rift development in the Northwestern Yangtze Block:
1165 evidence from the Hannan intrusive magmatism. Gondwana Res. 59, 27–42.

- 1166 <https://doi.org/10.1016/j.gr.2018.03.012>
- 1167 Maloof, A.C., Halverson, G.P., Kirschvink, J.L., Schrag, D.P., Weiss, B.P., Hoffman,
1168 P.F., 2006. Combined paleomagnetic, isotopic, and stratigraphic evidence for true
1169 polar wander from the Neoproterozoic Akademikerbreen Group, Svalbard,
1170 Norway. *Geol. Soc. Am. Bull.* 118, 1099–1124. <https://doi.org/10.1130/B25892.1>
- 1171 Mattauer, M., Matte, P., Malavieille, J., Tapponnier, P., Maluski, H., Xu, Z.Q., Lu,
1172 Y.L., Tang, Y.Q., 1985. Tectonics of the Qinling belt: build-up and evolution of
1173 eastern Asia. *Nature* 317, 496–500. <https://doi.org/10.1038/317496a0>
- 1174 McDonough, W.F., Sun, S.S., 1995. The composition of the Earth. *Chem. Geol.* 120,
1175 223–253. [https://doi.org/10.1016/0009-2541\(94\)00140-4](https://doi.org/10.1016/0009-2541(94)00140-4)
- 1176 Merdith, A.S., Collins, A.S., Williams, S.E., Pisarevsky, S., Foden, J.F., Archibald, D.,
1177 Blades, M.L., Alessio, B.L., Armistead, S., Plavsa, D., Clark, C., Müller, R.D.,
1178 2017. A full-plate global reconstruction of the Neoproterozoic. *Gondwana Res.*
1179 50, 84–134. <https://doi.org/10.1016/j.gr.2017.04.001>
- 1180 Middlemost, E.A.K., 1994. Naming materials in the magma/Igneous rock system.
1181 *Earth-Sci. Rev.* 37, 215–224. [https://doi.org/10.1016/0012-8252\(94\)90029-9](https://doi.org/10.1016/0012-8252(94)90029-9)
- 1182 Nie, H., Yao, J., Wan, X., Zhu, X.-Y., Siebel, W., Chen, F., 2016. Precambrian
1183 tectonothermal evolution of South Qinling and its affinity to the Yangtze Block:
1184 Evidence from zircon ages and Hf-Nd isotopic compositions of basement rocks.
1185 *Precambr. Res.* 286, 167–179. <https://doi.org/10.1016/j.precamres.2016.10.005>
- 1186 Nie, H., Ye, R.S., Cheng, H., Zhu, X.Y., Chen, F.K., 2019. Neoproterozoic intrusions
1187 along the northern margin of South Qinling, central China: Geochemistry, zircon
1188 ages, and tectonic implications. *Precambrian Research* 334, 105406.
1189 <https://doi.org/10.1016/j.precamres.2019.105406>
- 1190 Niu, B.G., He, Z.J., Ren, J.S., Wang, J., Deng, P., 2006. SHRIMP U-Pb ages of zircons
1191 from the intrusions in the western Douling-Xiaomaoling Uplift and their
1192 geological significances. *Geological Review* 52, 826–835 (in Chinese with
1193 English abstract).
- 1194 Niu, J., Li, Z.-X., Zhu, W., 2016. Palaeomagnetism and geochronology of mid-
1195 Neoproterozoic Yanbian dykes, South China: implications for a c. 820–800 Ma
1196 true polar wander event and the reconstruction of Rodinia. *Geol. Soc. (Lond.)*
1197 *Spec. Publ.* 424, 191–211. <https://doi.org/10.1144/SP424.11>
- 1198 Park, Y., Swanson-Hysell, N. L., Xian, H., Zhang, S., Condon, D. J., Fu, H.,
1199 Macdonald, F. A., 2021. A consistently high-latitude South China from 820 to
1200 780 Ma: Implications for exclusion from Rodinia and the feasibility of large-
1201 scale true polar wander. *Journal of Geophysical Research: Solid Earth*, 126,
1202 e2020JB021541. <https://doi.org/10.1029/2020JB021541>
- 1203 Pearson, D.M., MacLeod, D.R., Ducea, M.N Gehrels, G.E., Jonathan Patchett, P.,
1204 2017. Sediment underthrusting within a continental magmatic arc: Coast
1205 Mountains batholith, British Columbia. *Tectonics* 36, 2022–2043.
1206 <https://doi.org/10.1002/2017TC004594>
- 1207 Pei, X.Z., 1992. The feature and the tectonic setting of the flysch Formation in the
1208 Bikou area, the South Qinling. *J. Xi'an Coll. Geol.* 14, 42–49. (in Chinese with
1209 an English abstract).

- 1210 Peng, M., Wu, Y., Gao, S., et al. 2012a. Geochemistry, zircon U–Pb age and Hf
1211 isotope compositions of Paleoproterozoic aluminous A-type granites from the
1212 Kongling terrain, Yangtze Block: Constraints on petrogenesis and geologic
1213 implications, *Gondwana Res.*, 22, 140–151.
1214 <https://doi.org/10.1016/j.gr.2011.08.012>
- 1215 Peng, S.B., Kusky, T.M., Jiang, X.F., Wang, L., Wang, J.P., Deng, H., 2012b. Geology,
1216 geochemistry, and geochronology of the Miaowan ophiolite, Yangtze craton:
1217 implications for South China's amalgamation history with the Rodinian
1218 supercontinent. *Gondwana Res.* 21, 577–594.
1219 <https://doi.org/10.1016/j.gr.2011.07.010>
- 1220 Ping, X.Q., Zheng, J.P., Xiong, Q., Zhang, Z.H., Xia, B., 2014. Zircon U-Pb ages and
1221 Hf isotope characteristics of the granitic plutons in Bikou Terrane, northwestern
1222 Yangtze Block, and their geological significance. *J. Jilin Univ. Earth Sci. Ed.* 44,
1223 1200–1218. <http://xuebao.jlu.edu.cn/dxb/EN/Y2014/V44/I4/1200>
- 1224 Qin, K.L., Song, S.G., He, S.P., 1992. The geological characteristics of the Yudongzi
1225 granite-greensone terrain and its gold-bearing property in Mianluening area
1226 Shanxi. *Northwest Geosci.* 13 (1), 65–74 (in Chinese with English Abstract).
- 1227 Qiu, X.F., Ling, W.L., Liu, X.M., Kusky, T., Berkana, W., Zhang, Y.H., Gao, Y.J., Lu,
1228 S.S., Kuang, H., Liu, C.X., 2011. Recognition of Grenvillian volcanic suite in the
1229 Shennongjia region and its tectonic significance for the South China Craton.
1230 *Precambrian Res.* 191, 101–119. <https://doi.org/10.1016/j.precamres.2011.09.011>
- 1231 Rapela, C.W., Pankhurst, R.J., Fanning, C.M., Hervé, F., 2005. Pacific subduction
1232 coeval with the Karoo mantle plume: the Early Jurasssic Subcordilleran belt of
1233 northwestern Patagonia. *Geological Society, London, Special Publications*, 246,
1234 217–239. <https://doi.org/10.1144/GSL.SP.2005.246.01.07>
- 1235 Ratschbacher, L., Dingeldey, C.H., Miller, C.H., Hacker, B.R., McWilliams, M., 2004.
1236 Formation, subduction, and exhumation of Penninic oceanic crust in the Eastern
1237 Alps: Time constraints from $^{40}\text{Ar}/^{39}\text{Ar}$ geochronology, *Tectonophys.* 394, 155–
1238 170. <https://doi.org/10.1016/j.tecto.2004.08.003>
- 1239 Rickwood, P.C., 1989. Boundary lines within petrologic diagrams which use oxides of
1240 major and minor elements. *Lithos* 22, 247–263. [https://doi.org/10.1016/0024-4937\(89\)90028-5](https://doi.org/10.1016/0024-4937(89)90028-5)
- 1241 Rudnick, R.L., Gao, S., 2003. Composition of the continental crust. In: Holland, H.D.,
1242 Turekian, K.K. (Eds.), *Treatise on Geochemistry*. Pergamon, Oxford, pp. 1–64.
1243 <https://doi.org/10.1016/B0-08-043751-6/03016-4>
- 1244 Rumble, D., Giorgis, D., Ireland, T., Zhang, Z., Xu, H., Yui, T.F., Yang, J., Xu, Z.,
1245 Liou, J.G., 2002. Low $\delta^{18}\text{O}$ zircons, U-Pb dating, and the age of the
1246 Qinglongshan oxygen and hydrogen isotope anomaly near Donghai in Jiangsu
1247 Province, China. *Geochim. Cosmochim. Acta* 66, 2299–2306.
1248 [https://doi.org/10.1016/S0016-7037\(02\)00844-X](https://doi.org/10.1016/S0016-7037(02)00844-X)
- 1249 Rumble, D., Yui, T.F., 1998. The Qinglongshan oxygen and hydrogen isotope
1250 anomaly near Donghai in Jiangsu Province, China. *Geochim. Cosmochim. Acta*
1251 62, 3307–3321. [https://doi.org/10.1016/S0016-7037\(98\)00239-7](https://doi.org/10.1016/S0016-7037(98)00239-7)
- 1252 Saito, S., Tani, K., 2017. Transformation of juvenile Izu–Bonin–Mariana oceanic arc

- 1254 into mature continental crust: an example from the Neogene Izu collision zone
1255 granitoid plutons, Central Japan. *Lithos* 277, 228–240.
1256 <https://doi.org/10.1016/j.lithos.2016.07.035>
- 1257 Sauer, K.B., Gordon, S.M., Miller, R.B., Vervoort, J.D., Fisher, C.M., 2017. Transfer
1258 of metasupracrustal rocks to midcrustal depths in the North Cascades continental
1259 magmatic arc, Skagit Gneiss Complex, Washington. *Tectonics* 36, 3254–3276.
1260 <https://doi.org/10.1002/2017TC004728>
- 1261 Shaanxi, R.G.S., 1989. Regional Geology of Shaanxi Province (in Chinese).
1262 Geological Publishing House, Beijing.
- 1263 Shi, X.B., Deng, Q.Z., 2014. The Formation Age of the Granite-porphyry and Its
1264 Geological Significance in Shiyazi of Fang County. *Resources Environment &*
1265 *Engineering* 28, 835-840 (in Chinese with English abstract).
- 1266 Shi, Y., Liu, D., Zhang, Z., Miao, L., Zhang, F., Xue, H., 2007. SHRIMP Zircon U-Pb
1267 Dating of Gabbro and Granite from the Huashan Ophiolite, Qinling Orogenic
1268 Belt, China: Neoproterozoic Suture on the Northern Margin of the Yangtze
1269 Craton. *Acta Geol. Sin.* 81, 239-243. <https://doi.org/10.1111/j.1755-6724.2007.tb00947.x>
- 1270 Shu, L., Charvet, J., 1996. Kinematics and geochronology of the Proterozoic
1271 Dongxiang-Shexian ductile shear zone: with HP metamorphism and ophiolitic
1272 mélange (Jiangnan Region, South China). *Tectonophysics* 267, 291–302.
1273 [https://doi.org/10.1016/S0040-1951\(96\)00104-7](https://doi.org/10.1016/S0040-1951(96)00104-7)
- 1274 Su, C.Q., Hu, J.M., Li, Y., Liu, J.Q., 2006. The existence of two different tectonic
1275 attributes in Yaolinghe Group in South Qinling region. *Acta Petrologica et Min-*
1276 *eralogical* 25, 287–298 (in Chinese with English abstract).
- 1277 Sun, L., Wang, W., Pandit, M., Lu, G., Xue, E., Huang, B., Zhang, Y., Jin, W., Tian, Y.,
1278 2022. Geochemical and detrital zircon age constraints on Meso- to
1279 Neoproterozoic sedimentary basins in the southern Yangtze Block: Implications
1280 on Proterozoic geodynamics of South China and Rodinia configuration.
1281 *Precambrian Res.* 378, 106779. <https://doi.org/10.1016/j.precamres.2022.106779>
- 1282 Sun, W.H., Zhou, M.F., Gao, J.F., Yang, Y.H., Zhao, X.F., Zhao, J.H., 2009. Detrital
1283 zircon U-Pb geochronological and Lu-Hf isotopic constraints on the
1284 Precambrian magmatic and crustal evolution of the western Yangtze block, SW
1285 China. *Precambrian Res.* 172, 99–126.
1286 <https://doi.org/10.1016/j.precamres.2009.03.010>
- 1287 Sun, S.-S., McDonough, W.I., 1989. Chemical and isotopic systematics of oceanic
1288 basalts: implications for mantle composition and processes. In: Saunders, A.D.,
1289 Norry, M.J. (Eds.), *Magmatism in the Ocean Basins*. Special Publication.
1290 Geological Society of London, London, pp. 313–345.
1291 <https://doi.org/10.1144/gsl.sp.1989.042.01.19>
- 1292 Tao, H., Chen, X., Feng, H., et al., 1982. Strata classification and comparison for the
1293 ‘Xixiang group’, South Hanzhong. *Journal of Xi'an College of Geology*, 4, 1-
1294 698 (in Chinese).
- 1295 Tian, H., Li, H.K., Zhou, H.Y., Zhang, J., Zhang, K., Geng, J.Z., Xiang, Z.Q., Qu, L.S.,
1296 2017. Depositional age of the Huashan Group on the Northern margin of the
- 1297

- 1298 Yangtze Plate and Its Constraints on Breakup of the Rodinia supercontinent. *Acta*
1299 *Geologica Sinica* 91, 2387-2408 (in Chinese with English abstract).
- 1300 Valley, J.W., Kinny, P.D., Schulze, D.J., Spicuzza, M.J., 1998. Zircon megacrysts
1301 from kimberlite: oxygen isotope variability among mantle melts. *Contributions*
1302 to *Mineralogy and Petrology* 133, 1-11. <https://doi.org/10.1007/s004100050432>
- 1303 Wang, D.-B., Wang, B.-D., Yin, F.-G., Sun, Z.-M., Liao, S.-Y., Tang, Y., Luo, L., Liu,
1304 Z., 2019a. Petrogenesis and tectonic implications of Late Mesoproterozoic A1
1305 and A2-type felsic lavas from the Huili Group, southwestern Yangtze Block.
1306 *Geological Magazine* 156, 1425-1439.
1307 <https://doi.org/10.1017/S0016756818000882>
- 1308 Wang, D.S., Wang, Z.Q., Wu, Y.D., Wang, G., Zhang, Y.T., 2017a. Zircon SHRIMP U-
1309 Pb Age and Geochemical Characteristics of Syenogranite in the Suizhou Area,
1310 South Qinling. *Acta Geologica Sinica* 91, 1007-1021 (in Chinese with English
1311 abstract).
- 1312 Wang, J., Li, Z.X., 2003. History of Neoproterozoic rift basins in South China:
1313 implications for Rodinia break-up. *Precambrian Research* 122, 141-158.
1314 [https://doi.org/10.1016/S0301-9268\(02\)00209-7](https://doi.org/10.1016/S0301-9268(02)00209-7)
- 1315 Wang, M., Nebel, O., Wang, C.Y., 2016a. The flaw in the crustal “zircon archive”:
1316 Mixed hf isotope signatures record progressive contamination of late-stage liquid
1317 in mafic-ultramafic layered intrusions. *J. Petrol.* 57, 27–52.
1318 <https://doi.org/10.1093/petrology/egv072>
- 1319 Wang, M.X., Wang, C.Y., Zhao, J.H., 2013. Zircon U/Pb dating and Hf-O isotopes of
1320 the Zhouan ultramafic intrusion in the northern margin of the Yangtze Block, SW
1321 China: Constraints on the nature of mantle source and timing of the
1322 supercontinent Rodinia breakup. *Chinese Science Bulletin* 58, 777–787.
1323 <https://doi.org/10.1007/s11434-012-5435-1>
- 1324 Wang, Q., Wymanc, D., Li, Z., Bao, Z., Zhao, Z., Wang, Y., Jian, P., Yang, Y., Chen.,
1325 L., 2010. Petrology, geochronology and geochemistry of ca. 780 Ma A-type
1326 granites in South China: Petrogenesis and implications for crustal growth during
1327 the breakup of the supercontinent Rodinia. *Precambrian Research*, 178, 185-208.
1328 <https://doi.org/10.1016/j.precamres.2010.02.004>
- 1329 Wang, R., Xu, Z., Santosh, M., Zeng, B., 2021. Mid-Neoproterozoic magmatism in
1330 the northern margin of the Yangtze Block, South China: Implications for
1331 transition from subduction to post-collision. *Precambrian Res.* 354, 106073.
1332 <https://doi.org/10.1016/j.precamres.2020.106073>
- 1333 Wang, R.R., Xu, Z.Q., Santosh, M., 2019b. Neoproterozoic magmatism in the
1334 northern margin of the Yangtze Block, China: Implications for slab rollback in a
1335 subduction-related setting. *Precambrian Res.* 327, 176–195.
1336 <https://doi.org/10.1016/j.precamres.2019.03.003>
- 1337 Wang, R.R., Xu, Z.Q., Santosh, M., Xu, X.B., Deng, Q., Fu, X.H., 2017b. Middle
1338 Neoproterozoic (ca. 705–716 Ma) arc to rift transitional magmatism in the
1339 northern margin of the Yangtze Block: constraints from geochemistry, zircon U-
1340 Pb geochronology and Hf isotopes. *Journal of Geodynamics* 109, 59–74.
1341 <https://doi.org/10.1016/j.jog.2017.07.003>

- 1342 Wang, R.R., Xu, Z.Q., Santosh, M., Yao, Y., Gao, L.E., Liu, C.H., 2016b. Late
1343 Neoproterozoic magmatism in South Qinling, Central China: geochemistry,
1344 zircon U-Pb-Lu-Hf isotopes and tectonic implications. *Tectonophysics* 683, 43-
1345 61. <https://doi.org/10.1016/j.tecto.2016.05.050>
- 1346 Wang, T., Wang, Z.Q., Yan, Z., Yan, Q.R., Zhang, Y.L., Xiang, Z.J., 2009.
1347 Geochemical characteristic and zircon SHRIMP U-Pb dating of Sehe granite in
1348 Shanyang county, Shanxi province and its geological significance. *Acta
1349 Geologica Sinica* 83, 1657-1666 (in Chinese with English abstract).
- 1350 Wang, W., Liu, S.W., Feng, Y.F., Li, Q.F., Wu, F.H., Wang, Z.Q., Wang, R.T., Yang,
1351 P.T., 2012a. Chronology, petrogenesis and tectonic setting of the Neoproterozoic
1352 Tongchang dioritic pluton at the northwestern margin of the Yangtze Block:
1353 Constraints from geochemistry and zircon U-Pb-Hf isotopic systematics. *Gond.
1354 Res.* 22, 699-716. <https://doi.org/10.1016/j.gr.2011.11.015>
- 1355 Wang, W., Zhou, M.-F., 2012. Sedimentary records of the Yangtze Block (South
1356 China) and their correlation with equivalent Neoproterozoic sequences on
1357 adjacent continents. *Sediment. Geol.* 265-266, 126-142.
1358 <https://doi.org/10.1016/j.sedgeo.2012.04.003>
- 1359 Wang, W., Zhou, M.-F., Zhao, J.-H., Pandit, M.K., Zheng, J.-P., Liu, Z.-R., 2016c.
1360 Neoproterozoic active continental margin in the southeastern Yangtze Block of
1361 South China: evidence from the ca. 830-810 Ma sedimentary strata. *Sediment.
1362 Geol.* 342, 254-267. <https://doi.org/10.1016/j.sedgeo.2016.07.006>
- 1363 Wang, X.C., Li, X.H., Li, W.X., and Li, Z.X., 2007a. Ca.825 Ma komatiitic basalts in
1364 South China: First evidence for >1500 °C mantle melts by a Rodinian mantle
1365 plume: *Geology*, 35, 1103-1106. <https://doi.org/10.1130/G23878A.1>
- 1366 Wang, X.C., Li, X.H., Li, W.X., Li, Z.X., Liu, Y., Yang, Y.H., Liang, X.R., Tu, X.L.,
1367 2008. The Bikou basalts in the northwestern Yangtze block, South China:
1368 Remnants of 820-810 Ma continental flood basalts? *Bull. Geol. Soc. Am.* 120,
1369 1478-1492. <https://doi.org/10.1130/B26310.1>
- 1370 Wang, X.-C., Li, X.-H., Li, Z.-X., Li, Q.-L., Tang, G.-Q., Gao, Y.-Y., Zhang, Q.-R.,
1371 Liu, Y., 2012b. Episodic Precambrian crust growth: Evidence from U-Pb ages
1372 and Hf-O isotopes of zircon in the Nanhua Basin, central South China.
1373 *Precambrian Res.* 222-223, 386-403.
1374 <https://doi.org/10.1016/j.precamres.2011.06.001>
- 1375 Wang, X.L., Zhou, J.C., Qiu, J.S., Gao, J.F., 2004. Geochemistry of the Meso- to
1376 Neoproterozoic basic-acid rocks from Hunan Province, South China:
1377 implications for the evolution of the western Jiangnan orogen. *Precambrian
1378 Research* 135, 79-103. <https://doi.org/10.1016/j.precamres.2004.07.006>
- 1379 Wang, X.L., Zhou, J.C., Qiu, J.S., Zhang, W.L., Liu, X.M., Zhang, G.L., 2006. LA-
1380 ICP-MS U-Pb zircon geochronology of the Neoproterozoic igneous rocks from
1381 Northern Guangxi, South China: Implications for tectonic evolution.
1382 *Precambrian Res.* 145, 111-130. <https://doi.org/10.1016/j.precamres.2005.11.014>
- 1383 Wang, X.L., Zhou, J.C., Griffin, W.L., Wang, R.C., Qiu, J.S., O'Reilly, S.Y., Xu, X.S.,
1384 Liu, X.M., Zhang, G.L., 2007b. Detrital zircon geochronology of Precambrian
1385 basement sequences in the Jiangnan orogen: dating the assembly of the Yangtze

- 1386 and Cathaysia blocks. *Precambr. Res.* 159, 117–131.
1387 <https://doi.org/10.1016/j.precamres.2007.06.005>
- 1388 Wang, X.L., Zhou, J.C., Griffin, W.L., Zhao, G.C., Yu, J.H., Qiu, J.S., Zhang, Y.J.,
1389 Xing, G.F., 2014. Geochemical zonation across a Neoproterozoic orogenic belt:
1390 Isotopic evidence from granitoids and metasedimentary rocks of the Jiangnan
1391 orogeny, China. *Precambr. Res.* 242, 154–171.
1392 <https://doi.org/10.1016/j.precamres.2013.12.023>
- 1393 Wang, Y.-J., Zhu, W.-G., Huang, H.-Q., Zhong, H., Bai, Z.-J., Fan, H.-P., Yang, Y.-J.,
1394 2019c. Ca. 1.04 Ga hot Grenville granites in the western Yangtze Block,
1395 southwest China. *Precambrian Res.* 328, 217-234.
1396 <https://doi.org/10.1016/j.precamres.2019.04.024>
- 1397 Wei, G., Zou, G., Pan, W., Luo, M., Ma, Z., Mao, Q., Yu, X., 2019. Zircon U-Pb age,
1398 geochemical characteristics and tecnic significance of the K-feldspar granite in
1399 Guanwushan area, northern margin of the Yangtze plate. *J. Mineral Petrol.* 39,
1400 14-24 (in Chinese with English abstract).
- 1401 Wu, F.F., Wang, Z.Q., Wang, T., Yan, Z., Chen, L., 2012. SHRIMP zircons U-Pb ages
1402 and geochemical characteristics of the Banbanshan K-feldspar granite in
1403 Shanyang, Southern Qinling orogenic belt. *Journal of Mineral Petrology* 32, 63-
1404 73 (in Chinese with English abstract).
- 1405 Wu, P., Zhang, S.-B., Zheng, Y.-F., Fu, B., Liang, T., 2019. Amalgamation of South
1406 China into Rodinia during the Grenvillian accretionary orogeny: Geochemical
1407 evidence from Early Neoproterozoic igneous rocks in the northern margin of the
1408 South China Block. *Precambrian Res.* 321, 221-243.
1409 <https://doi.org/10.1016/j.precamres.2018.12.015>
- 1410 Wu, P., Zhang, S.-B., Zheng, Y.-F., Li, Q.-L., Li, Z.-X., Sun, F.-Y., 2020. The
1411 occurrence of Neoproterozoic low $\delta^{18}\text{O}$ igneous rocks in the northwestern
1412 margin of the South China Block: Implications for the Rodinia configuration.
1413 *Precambrian Research* 347, 105841.
1414 <https://doi.org/10.1016/j.precamres.2020.105841>
- 1415 Wu, P., Zhang S.B., Zheng Y.F., Fu B., Li Q.L., Yang Y.H., Hu Z., Liang T., 2021. The
1416 accretion history of the South China Block at its northwest margin in the
1417 Neoproterozoic: records from the Changba Complex in the Mian-Lue Zone.
1418 *Precambrian Research* 352, 106006.
1419 <https://doi.org/10.1016/j.precamres.2020.106006>
- 1420 Wu, P., Zhang, S.B., Li, Z.X., Wu, Y.B., Zheng, Y.F., 2023. Secular change in the
1421 nature of mantle and tectonic evolution of northwestern margin of the Yangtze
1422 Block during Neoproterozoic: Constraints from the mafic intrusions and
1423 associated granitoids of the Hannan and Xiaomoling complexes. *Precambrian*
1424 *Res.* 393, 107094. <https://doi.org/10.1016/j.precamres.2023.107094>
- 1425 Wu, T., Wang, X., Li, W., et al., 2019. Petrogenesis of the ca. 820-810 Ma felsic
1426 volcanic rocks in the Bikou Group: Implications for the tectonic setting of the
1427 western margin of the Yangtze Block. *Precambrian research*, 331, 105370.
1428 <https://doi.org/10.1016/j.precamres.2019.105370>
- 1429 Wu, W.N., Jiang, T., Xu, Q., Zhao, X.M., Zhao, L., Qiu, X.F., 2021b. Recognition of

- 1430 Late Neoproterozoic bimodal volcanic rocks from the Yaolinghe Formation in
1431 the Suizao terrane, South Qinling block: Constraints on the continental rifting of
1432 the northern margin of Yangtze craton. *Geol. Bull. China* 40, 920–929 (in
1433 Chinese with English abstract).
- 1434 Wu, Y., Zheng, Y., Gao, S., Jiao, W., Liu, Y., 2008. Zircon U–Pb age and trace element
1435 evidence for Paleoproterozoic granulite-facies metamorphism and Archean
1436 crustal rocks in the Dabie Orogen, *Lithos*, 101, 308–322.
1437 <https://doi.org/10.1016/j.lithos.2007.07.008>
- 1438 Wu, Y., S. Gao, H.-J. Gong, H. Xiang, W.-F. Jiao, S.-H. Yang, Y.-S. Liu, Yuan, H.-L.,
1439 2009. Zircon U–Pb age, trace element and Hf isotope composition of Kongling
1440 terrane in the Yangtze Craton: Refining the timing of Paleoproterozoic high-
1441 grade metamorphism, *J. Metamor. Geol.* 27, 461–477.
1442 <https://doi.org/10.1111/j.1525-1314.2009.00826.x>
- 1443 Wu, Y., Zhou, G., Gao, S., Liu, X., Qin, Z., Wang, H., Yang, J., Yang, S., 2014.
1444 Petrogenesis of Neoarchean TTG rocks in the Yangtze Craton and its implication
1445 for the formation of Archean TTGs. *Precambr. Res.* 254, 73–86.
1446 <https://doi.org/10.1016/j.precamres.2014.08.004>
- 1447 Wu, Y.-B., Gao, S., Zhang, H., Zheng, J., Liu, X., Wang, H., Gong, H., Zhou, L., Yuan,
1448 H., 2012. Geochemistry and zircon U–Pb geochronology of Paleoproterozoic arc
1449 related granitoid in the Northwestern Yangtze Block and its geological
1450 implications. *Precambrian Res.* 200–203, 26–37.
1451 <https://doi.org/10.1016/j.precamres.2011.12.015>
- 1452 Xia, L., Xia, Z., Li, X., Ma, Z., Xu, X., 2008. Petrogenesis of the Yaolinghe Group,
1453 Yunxi Group, Wudangshan Group volcanic rocks and basic dyke swarms from
1454 eastern part of the South Qinling Mountains. *Northwestern Geology* 41, 1–29 (in
1455 Chinese with English abstract).
- 1456 Xia, L.Q., Xia, Z.C., Ma, Z.P., Xu, X.Y., Li, X.M., 2009. Petrogenesis of volcanic
1457 rocks from Xixiang Group in middle part of South Qinling Mountains.
1458 *Northwestern Geology* 42 (1), 1–37 (in Chinese with English abstract).
- 1459 Xia, L.Q., Xia, Z.C., Xu, X.Y., 1996a. Properties of middle-late Proterozoic volcanic
1460 rocks in South Qinling and Precambrian continental break-up. *Science in China*
1461 (Series D) 39, 256–265. <https://doi.org/10.1360/yd1996-39-3-256>
- 1462 Xia, L.Q., Xia, Z.C., Xu, X.Y., 1996b. The confirmation of continental flood basalt of
1463 the Proterozoic Xixiang Group in the south Qinling Mountains and its geological
1464 implications. *Geological Review* 42 (6), 513–522 (in Chinese with English
1465 abstract).
- 1466 Xian, H., Zhang, S., Li, H., Xiao, Q., Chang, L., Yang, T., Wu, H., 2019. How did
1467 South China connect to and separate from Gondwana? New paleomagnetic
1468 constraints from the Middle Devonian Red Beds in South China. *Geophys. Res.*
1469 Lett. 46, 7371–7378. <https://doi.org/10.1029/2019GL083123>
- 1470 Xian, H., Zhang, S., Li, H., Yang, T., Wu, H., 2020. Geochronological and
1471 palaeomagnetic investigation of the Madiyi Formation, lower Banxi Group,
1472 South China: Implications for Rodinia reconstruction. *Precambrian Res.* 336,
1473 105494. <https://doi.org/10.1016/j.precamres.2019.105494>

- 1474 Xiao, L., Zhang, H.F., Ni, P.Z., Xiang, H., Liu, X.M., 2007. LA-ICP-MS U-Pb zircon
1475 geochronology of early Neoproterozoic mafic-intermediat intrusions from NW
1476 margin of the Yangtze Block, South China: Implication for tectonic evolution.
1477 *Precambr. Res.* 154, 221–235. <https://doi.org/10.1016/j.precamres.2006.12.013>
- 1478 Xu, D., Gu, X., Li, P., Chen, G., Xia, B., Bachlinski, R., He, Z., Fu, G., 2007.
1479 Mesoproterozoic–Neoproterozoic transition: geochemistry, provenance and
1480 tectonic setting of clastic sedimentary rocks on the SE margin of the Yangtze
1481 Block, South China. *J. Asian Earth Sci.* 29, 637–650.
1482 <https://doi.org/10.1016/j.jseas.2006.04.006>
- 1483 Xu, T., Pei, X., Li, R., Liu, C., Chen Y., Li, Z., Pei, L., Zuo, W., 2017. Ages and
1484 Geochemical Features of the Heigouxia Volcanic Rocks in the Mianxian—
1485 Lüeyang Area of South Qinling Orogen: Evidence for Existence and Subduction
1486 of Neoproterozoic Mianxian—Lüeyang Ocean. *Geological Review*, 63, 375-394
1487 (in Chinese with English abstract).
- 1488 Xu, X.Y., Chen, J.L., Li, X.M., Ma, Z.P., Wang, H.L., Li, P., Li, T., 2009a.
1489 Geochemical constrains on the petrogenesis and tectonic setting discrimination
1490 of volcanic rocks from the Baimianxia and the Sanwan Formations. *Acta Geol.*
1491 *Sin.* 11, 1703–1718 (in Chinese with English Abstract).
- 1492 Xu, X.Y., Chen, J.L., Li, X.M., Ma, Z.P., Wang, H.L., Xia, L.Q., Xia, Z.C., Li, P.,
1493 2010. Geochemistry and petrogenesis of volcanic rocks from Sanlangpu
1494 Formation and Dashigou Formation. *Acta Petrol. Sin.* 26, 617–632 (in Chinese
1495 with English Abstract).
- 1496 Xu, X.Y., Xia, L.Q., Chen, J.L., Ma, Z.P., Li, X.M., Xia, Z.C., Wang, H.L., 2009b.
1497 Zircon U-Pb dating and geochemical study of volcanic rocks Group in northern
1498 margin of Yangtze Plate in from Sunjiahe Formation of Xixiang. *Acta Petrol. Sin.*
1499 25, 3309–3326 (Chinese with English abstract).
- 1500 Xu, Y., Yang, K.G., Polat, A., Yang, Z.N., 2016. The ~860 Ma mafic dikes and
1501 granitoids from the northern margin of the Yangtze Block, China: A record of
1502 oceanic subduction in the early Neoproterozoic. *Precambrian Research* 275,
1503 310–331. <https://doi.org/10.1016/j.precamres.2016.01.021>
- 1504 Xue, F., Kroner, A., Reischmann, T., Lerch, F., 1996. Palaeozoic pre- and post-
1505 collision calc-alkaline magmatism in the Qinling orogenic belt, central China, as
1506 documented by zircon ages on granitoid rock. *Journal of the Geological Society.*
1507 London, 153, 409-417. <https://doi.org/10.1144/gsjgs.153.3.0409>
- 1508 Xue, H.M., Ma, F., Song, Y.Q., 2011. Geochemistry and SHRIMP zircon U–Pb data
1509 of Neoproterozoicmeta-magmatic rocks in the Suizhou–Zaoyang area, northern
1510 margin of the Yangtze Craton, Central China. *Acta Petrologica Sinica* 27, 1116–
1511 1130 (in Chinese with English abstract).
- 1512 Yan M., Liu S.W., Li Q.G., Yang P.T., Wang W., Guo R.R., Bai X., Deng Z.B., 2014.
1513 LA-ICP-MS zircon U-Pb chronology and Lu-Hf isotopic features of the
1514 Mihunzhen pluton in the South Qinling tectonic belt. *Acta Petrologica Sinica*. 30,
1515 390-400. (in Chinese with English abstract).
- 1516 Yan, L.Q., 1959. Basic achievements of regional geological surveying and
1517 reconnaissance surveying in Qingling Mountains. *Geological Monthly Magazine*,

- 1518 (11): 32-39 (in Chinese).
- 1519 Yan, Q.R., Andrew, D.H., Wang, Z.Q., Yan, Z., Peter, A.D., Wang, T., Liu, D.Y., Song,
1520 B., Jiang, C.F., 2004a. Geochemistry and tectonic setting of the Bikou volcanic
1521 terrane on the northern margin of the Yangtze plate. *Acta Petrol. Mineral.* 23, 1–
1522 11 (in Chinese with an English abstract).
- 1523 Yan, Q., A. D. Hanson, Z. Wang, P. A. Druschke, Z. Yan, T. Wang, and D. Liu 2004b,
1524 Neoproterozoic subduction and rifting on the northern margin of the Yangtze
1525 plate, China: Implications for Rodinia reconstruction, *Int. Geol. Rev.*, 46, 817–
1526 832. <https://doi.org/10.2747/0020-6814.46.9.817>
- 1527 Yan, Z., Wang, Z., Chen, J., Yan, Q., Wang, T., 2010. Detrital record of
1528 Neoproterozoic arc-magmatism along the NW margin of the Yangtze Block,
1529 China: U–Pb geochronology and petrography of sandstones. *Journal of Asian
1530 Earth Sciences* 37, 322-334. <https://doi.org/10.1016/j.jseaes.2009.09.001>
- 1531 Yang, J.-H., Wu, F.-Y., Wilde, S.A., Xie, L.-W., Yang, Y.-H., Liu, X.-M., 2007. Tracing
1532 magma mixing in granite genesis: in situ U–Pb dating and Hf-isotope analysis of
1533 zircons. *Contrib. Mineral. Petrol.* 153, 177–190. <https://doi.org/10.1007/s00410-006-0139-7>
- 1535 Yang, P.T., Liu, S.W., Li, Q.G., Wang, Z.Q., Wang, W., Bai, X., 2012. Emplacing age
1536 of the Tiewadian pluton in the South Qinling tectonic belt and its geological
1537 implications. *Acta Geologica Sinica* 86, 1525–1540 (in Chinese with English
1538 abstract).
- 1539 Yang, Y.-N., Wang, X.-C., Li, Q.-L., Li, X.-H., 2016. Integrated in situ U-Pb age and
1540 Hf-O analyses of zircon from Suixian Group in northern Yangtze: New insights
1541 into the Neoproterozoic low- $\delta^{18}\text{O}$ magmas in the South China Block.
1542 *Precambrian Res.* 273, 151–164.
1543 <https://doi.org/10.1016/j.precamres.2015.12.008>
- 1544 Yang, Z.J., Wei, L., Cai, W.C., Yang, W.B., Zhou, B., 2020. LA-ICP-MS zircon U-Pb
1545 ages and geochemical characteristics of the Banbanshan monzogranite in
1546 Southern Qinling orogenic belt and their geological significance. *Acta
1547 Petrologica et Mineralogica* 39, 539-551 (in Chinese with English abstract).
- 1548 Yang, Z.-N., Yang, K.-G., Polat, A., Xu, Y., 2018. Early crustal evolution of the
1549 eastern Yangtze Block: evidence from detrital zircon U-Pb ages and Hf isotopic
1550 composition of the Neoproterozoic Huashan Group in the Dahongshan area.
1551 *Precambr. Res.* 309, 248–270. <https://doi.org/10.1016/j.precamres.2017.05.011>
- 1552 Yao, J., Shu, L., Cawood, P.A., Li, J., 2016. Delineating and characterizing the
1553 boundary of the Cathaysia Block and the Jiangnan orogenic belt in South China.
1554 *Precambr. Res.* 275, 265–277. <https://doi.org/10.1016/j.precamres.2016.01.023>
- 1555 Yin, C.Q., Lin, S.F., Davis, D.W., Zhao, G.C., Xiao, W.J., Li, L.M., He, Y.H., 2013.
1556 2.1-1.85 Ga tectonic events in the Yangtze Block, South China: petrological and
1557 geochronological evidence from the Kongling Complex and implications for the
1558 reconstruction of supercontinent Columbia. *Lithos* 182, 200–210.
1559 <https://doi.org/10.1016/j.lithos.2013.10.012>
- 1560 Yui, T.-F., Rumble, D., Lo, C.-H., 1995. Unusually low $\delta^{18}\text{O}$ ultra-high-pressure
1561 metamorphic rocks from the Sulu Terrain, eastern China. *Geochim. Cosmochim.*

- 1562 Acta 59, 2859–2864. [https://doi.org/10.1016/0016-7037\(95\)00161-R](https://doi.org/10.1016/0016-7037(95)00161-R)
- 1563 Zhang, C.L., Li, M., Wang, T., Yuan, H.L., Yan, Y.X., Liu, X.M., Wang, J.Q., Liu, Y.,
1564 2004a. U-Pb zircon geochronology and geochemistry of granitoids in the
1565 Douling Group in the eastern Qinling. Acta Geologica Sinica 78, 83–95 (in
1566 Chinese with English abstract).
- 1567 Zhang, J., Zhang, H.F., Li, L., 2018. Neoproterozoic tectonic transition in the South
1568 Qinling Belt: New constraints from geochemistry and zircon U–Pb–Hf isotopes
1569 of diorites from the Douling Complex. Precambrian Research 306, 112-128.
1570 <https://doi.org/10.1016/j.precamres.2017.12.043>
- 1571 Zhang, R., Sun, Y., Zhang, X., Ao, W., Santosh, M., 2016. Neoproterozoic magmatic
1572 events in the South Qinling Belt, China: Implications for amalgamation and
1573 breakup of the Rodinia supercontinent. Gondwana Research 30, 6-23.
1574 <https://doi.org/10.1016/j.gr.2015.06.015>
- 1575 Zhang, S., Zhang, Z., Song, B., Tang, S., Zhao, Z., Wang, J., 2004b. On the existence
1576 of Neoarchean materials in the Douling complex, eastern Qinling - Evidence
1577 from U–Pb SHRIMP and Sm–Nd geochronology. Acta Geol. Sinica, 78, 800–
1578 806 (in Chinese with English abstract).
- 1579 Zhang, S., Y. Zheng, Y., Wu, Y., Zhao, Z., Gao, S., Wu, F., 2006. Zircon isotope
1580 evidence for ≥ 3.5 Ga continental crust in the Yangtze craton of China,
1581 Precambrian Res., 146, 16–34. <https://doi.org/10.1016/j.precamres.2006.01.002>
- 1582 Zhang, S., Zheng, Y., Zhao, Z., Wu, Y., Yuan, H., Wu, F., 2008. Neoproterozoic
1583 anatexis of Archean lithosphere: Geochemical evidence from felsic to mafic
1584 intrusions at Xiaofeng in the Yangtze Gorge, South China, Precambrian Res.,
1585 163, 210–238. <https://doi.org/10.1016/j.precamres.2007.12.003>
- 1586 Zhang, S.B., Zheng, Y.-F., 2013a. Formation and evolution of Precambrian
1587 continental lithosphere in South China. Gondwana Research 23, 1241-1260.
1588 <https://doi.org/10.1016/j.gr.2012.09.005>
- 1589 Zhang, S.B., Zheng, Y.F., 2013b. Time and space of Neoproterozoic low- $\delta^{18}\text{O}$
1590 magmatic rocks in South China. Chin. Sci. Bull., 58, 2344–2350 (in Chinese
1591 with English abstract).
- 1592 Zhang, S.B., Zheng, Y.-F., Wu, P., He, Q., Rong, W., Fu, B., Yang, Y.-H., Liang, T.,
1593 2020. The nature of subduction system in the Neoarchean: Magmatic records
1594 from the northern Yangtze Craton, South China. Precambrian Research 347,
1595 105834. <https://doi.org/10.1016/j.precamres.2020.105834>
- 1596 Zhang, W.F., Xu, D.L., Peng, L.H., Deng, X., Liu, H., Jin, X.B., Tan, J., 2018. The
1597 Discovery and Geological Significance of the Neoproterozoic A1-type Granite in
1598 the Pailou Area, Wudang Uplift. Earth Science 43, 2389-2403 (in Chinese with
1599 English abstract).
- 1600 Zhang, X., Xu, X.Y., Song, G.S., Wang, H.L., Chen, J.L., Li, T., 2010. Zircon LA-
1601 ICP-MS UPb dating and significance of Yudongzi Group deformation granite
1602 from Lueyang area, western Qinling China. Geological Bulletin of China 4 (29),
1603 510–517 (in Chinese with English abstract).
- 1604 Zhang, Y.Q., Zhang, J., Li, H.K., Lu, S.N., 2013. Zircon U-Pb Geochronology of the
1605 Meta-Acidic Volcanic Rocks from the Wudangshan Group, Southern Qinling

- 1606 Moutains, Central China. *Acta Geologica Sinica* 87, 922-930 (in Chinese with
1607 English abstract).
- 1608 Zhang, Z.Q., Zhang, G.W., Tang, S.H., Wang, J.H., 2001. On the age of metamorphic
1609 rocks of the Yudongzi Group and the Archean crystalline basement of the
1610 Qinling orogen. *Acta Geol. Sin.* 75, 198–204 (in Chinese with English abstract).
- 1611 Zhao, F.Q., Zhao, W.P., Zhuo, Y.C., Li, Z.H., Xue, K.Q., 2006. U-Pb geochronology
1612 of Neoproterozoic magmatic rocks in Hanzhong, southern Shaanxi, China. *Geol.*
1613 *Bull. Chin.* 25, 383–388. (In Chinese with English Abstract).
- 1614 Zhao, G., Cawood, P.A., 1999. Tectonothermal evolution of the Mayuan Assemblage
1615 in the Cathaysia Block; implications for Neoproterozoic collision-related
1616 assembly of the South China Craton: *Ameri. J. Sci.* 299, 309–339.
<https://doi.org/10.2475/ajs.299.4.309>
- 1618 Zhao, G.C., Cawood, P.A., 2012. Precambrian geology of China. *Precambrian Res.*
1619 222-223, 13-54. <https://doi.org/10.1016/j.precamres.2012.09.017>
- 1620 Zhao, J.-H., Asimow, P.D., 2018. Formation and Evolution of a Magmatic System in a
1621 Rifting Continental Margin: Neoproterozoic Arc- and MORB-like Dike Swarms
1622 in South China. *Journal of Petrology* 59, 1811-1844.
<https://doi.org/10.1093/petrology/egy080>
- 1624 Zhao, J.H., Zhou, M.F., 2008. Neoproterozoic adakitic suite at the northwestern
1625 margin of the Yangtze Block, China: evidence for partial melting of thickened
1626 lower crust and secular crustal evolution. *Lithos* 104, 231–248.
<https://doi.org/10.1016/j.lithos.2007.12.009>
- 1628 Zhao, J.H., Zhou, M.F., 2009a. Secular evolution of the Neoproterozoic lithospheric
1629 mantle underneath the northern margin of the Yangtze Block, South China.
1630 *Lithos* 107, 152–168. <https://doi.org/10.1016/j.lithos.2008.09.017>
- 1631 Zhao, J.H., Zhou, M.F., 2009b. Melting of newly formed mafic crust for the formation
1632 of Neoproterozoic I-type granite in the Hannan Region, South China. *J. Geol.*
1633 117, 54–70. <https://doi.org/10.1086/593321>
- 1634 Zhao, J.-H., Zhou, M.-F., and Zheng, J.-P., 2010a. Metasomatic mantle source and
1635 crustal contamination for the formation of the Neoproterozoic mafic dike swarm
1636 in the northern Yangtze Block, South China. *Lithos* 115, 177-189.
<https://doi.org/10.1016/j.lithos.2009.12.001>
- 1638 Zhao, J.-H., Zhou, M.-F., Yan, D.-P., Yang, Y.-H., Sun, M., 2008. Zircon Lu-Hf
1639 isotopic constraints on Neoproterozoic subduction-related crustal growth along
1640 the western margin of the Yangtze Block, South China. *Precambrian Research*
1641 163, 189–209. <https://doi.org/10.1016/j.precamres.2007.11.003>
- 1642 Zhao, J.H., Zhou, M.F., Yan, D.P., Zheng, J.P., Li, J.W., 2011. Reappraisal of the ages
1643 of Neoproterozoic strata in South China: No connection with the Grenvillian
1644 orogeny. *Geology* 39, 299-302. <https://doi.org/10.1130/G31701.1>
- 1645 Zhao, J.H., Zhou, M.F., Zheng, J.P., Fang, S.M., 2010b. Neoproterozoic crustal
1646 growth and reworking of the Northwestern Yangtze Block: constraints from the
1647 Xixiang dioritic intrusion, South China. *Lithos* 120, 439–452.
<https://doi.org/10.1016/j.lithos.2010.09.005>
- 1649 Zhao, J.-H., Nebel, O., Johnson, T.E., 2021. Formation and Evolution of a

- 1650 Neoproterozoic Continental Magmatic Arc. *J. Petrol.* 62, 1-53.
1651 <https://doi.org/10.1093/petrology/egab029>
- 1652 Zhao, L., Li, Y., Rong, C., Li, F., Xiang, H., Zheng, J., Brouwer, F., 2022.
1653 Geochemical and zircon U-Pb-Hf isotopic study of volcanic rocks from the
1654 Yaolinghe Group, South Qinling orogenic belt, China: Constraints on the
1655 assembly and breakup of Rodinia. *Precambrian Research*, 371, 106603.
1656 <https://doi.org/10.1016/j.precamres.2022.106603>
- 1657 Zheng, Y., Fu, B., Gong, B., Li, L., 2003. Stable isotope geochemistry of ultrahigh
1658 pressure metamorphic rocks from the Dabie-Sulu orogen in China: Implications
1659 for geodynamics and fluid regime, *Earth-Sci. Rev.*, 62, 105–161.
1660 [https://doi.org/10.1016/S0012-8252\(02\)00133-2](https://doi.org/10.1016/S0012-8252(02)00133-2)
- 1661 Zheng, Y., Wu, Y., Chen, F., Gong, B., Li, L., Zhao, Z., 2004. Zircon U-Pb and oxygen
1662 isotope evidence for a large-scale ^{18}O depletion event in igneous rocks during the
1663 Neoproterozoic, *Geochim. Cosmochim. Acta*, 68, 4145–4165.
1664 <https://doi.org/10.1016/j.gca.2004.01.007>
- 1665 Zheng, Y., Z. Zhao, Y. Wu, S. Zhang, X. Liu, and Wu, F., 2006. Zircon U–Pb age, Hf
1666 and O isotope constraints on protolith origin of ultrahigh-pressure eclogite and
1667 gneiss in the Dabie orogen, *Chem. Geol.*, 231, 135–158.
1668 <https://doi.org/10.1016/j.chemgeo.2006.01.005>
- 1669 Zheng, Y.-F., Wu, R.-X., Wu, Y.-B., Zhang, S.-B., Yuan, H., Wu, F.-Y., 2008. Rift
1670 melting of juvenile arc-derived crust: geochemical evidence from
1671 Neoproterozoic volcanic and granitic rocks in the Jiangnan Orogen. South China.
1672 *Precambrian Res.* 163, 351–383.
1673 <https://doi.org/10.1016/j.precamres.2008.01.004>
- 1674 Zheng, Y.F., Wu, Y.B., Gong, B., Chen, R.X., Tang, J., Zhao, Z.F., 2007. Tectonic
1675 driving of Neoproterozoic glaciations: evidence from extreme oxygen isotope
1676 signature of meteoric water in granite. *Earth and Planetary Science Letters* 256,
1677 196–210. <https://doi.org/10.1016/j.epsl.2007.01.026>
- 1678 Zhou, G., Wu, Y., Li, L., Zhang, W., Zheng, J., Wang, H., Yang, S., 2018a.
1679 Identification of ca. 2.65 Ga TTGs in the Yudongzi complex and its implications
1680 for the early evolution of the Yangtze Block. *Precambr. Res.* 314, 240–263.
1681 <https://doi.org/10.1016/j.precamres.2018.06.011>
- 1682 Zhou, G.Y., Wu, Y.B., Zhang, W.X., He, Y., 2019. Circa 900 Ma low $\delta^{18}\text{O}$ A-type
1683 rhyolite in the northern Yangtze Block: Genesis and geological significance.
1684 *Precambr. Res.* 324, 155–169. <https://doi.org/10.1016/j.precamres.2019.01.015>
- 1685 Zhou, J.-L., Li, X.-H., Tang, G.-Q., Gao, B.-Y., Bao, Z.-A., Ling, X.-X., Wu, L.-G., Lu,
1686 K., Zhu, Y.-S., Liao, X., 2018b. Ca. 890 Ma magmatism in the northwest Yangtze
1687 block, South China: SIMS U-Pb dating, in-situ Hf-O isotopes, and tectonic
1688 implications. *Journal of Asian Earth Sciences* 151, 101-111.
1689 <https://doi.org/10.1016/j.jseae.2017.10.029>
- 1690 Zhou, M.F., Kennedy, A.K., Sun, M., Malpas, J., Lesher, C.M., 2002a.
1691 Neoproterozoic arc-related mafic intrusions along the Northern Margin of South
1692 China: implications for the Accretion of Rodinia. *J. Geol.* 110, 611-618.
1693 <https://doi.org/10.1086/341762>

- 1694 Zhou, M.F., Ma, Y.X., Yan, D.P., Xia, X.P., Zhao, J.H., Sun, M., 2006a. The Yanbian
1695 terrane (Southern Sichuan Province, SW China): A neoproterozoic arc
1696 assemblage in the western margin of the Yangtze block. *The Yanbian terrane*
1697 (Southern Sichuan Province, SW China): a neoproterozoic arc assemblage in the
1698 western margin of the Yangtze block. *Precambrian Research* 144, 19–38.
1699 <https://doi.org/10.1016/j.precamres.2005.11.002>
- 1700 Zhou, M.F., Yan, D.P., Kennedy, A.K., Li, Y., Ding, J., 2002b. SHRIMP U–Pb zircon
1701 geochronological and geochemical evidence for Neoproterozoic arc-magmatism
1702 along the western margin of the Yangtze Block, South China. *Earth and*
1703 *Planetary Science Letters* 196, 51–67. [https://doi.org/10.1016/S0012-821X\(01\)00595-7](https://doi.org/10.1016/S0012-821X(01)00595-7)
- 1704 Zhou, M.F., Yan, D.P., Wang, C.L., Qi, L., Kennedy, A.K., 2006b. Subduction-related
1705 origin of the 750 Ma Xuelongbao adakitic complex (Sichuan Province, China):
1706 Implications for the tectonic setting of the giant Neoproterozoic magmatic event
1707 in South China. *Earth and Planetary Science Letters* 248, 286–300.
1708 <https://doi.org/10.1016/j.epsl.2006.05.032>
- 1709 Zhou, M.F., Zhao, J.H., Xia, X.P., Sun, W.H., Yan, D.P., 2007. Comment on
1710 “Revisiting the “Yanbian Terrane”: implications for Neoproterozoic tectonic
1711 evolution of the western Yangtze Block, South China” [Li et al. (2006)].
1712 *Precambrian Res.* 155, 153–157. <https://doi.org/10.1016/j.precamres.2006.11.013>
- 1713 Zhu, W.-G., Zhong, H., Li, Z.-X., Bai, Z.-J., Yang, Y.-J., 2016. SIMS zircon U–Pb
1714 ages, geochemistry and Nd–Hf isotopes of ca. 1.0 Ga mafic dykes and volcanic
1715 rocks in the Huili area, SW China: Origin and tectonic significance. *Precambrian*
1716 *Res.* 273, 67–89. <https://doi.org/10.1016/j.precamres.2015.12.011>
- 1717 Zhu, X., Long, X.P., Yang, X.X., Wang, J.Y., 2018. The formation temperature of
1718 Neoproterozoic magmatic intrusions in the Hannan area and its geological
1719 significance. *Chinese J. Geol.* 53, 1000–1026 (in Chinese with English abstract).
- 1720 Zhu, X.Y., Chen, F.K., Liu, B.X., Zhang, H., Zhai, M.G., 2015. Geochemistry and
1721 zircon ages of mafic dikes in the South Qinling, central China: evidence for late
1722 Neoproterozoic continental rifting in the northern Yangtze Block. *International*
1723 *Journal of Earth Sciences* 104, 27–44. <https://doi.org/10.1007/s00531-014-1056-z>
- 1724 Zhu, X.Y., Chen, F.K., Nie, H., Siebel, W., Yang, Y.Z., Xue, Y.Y., Zhai, M.G., 2014.
1725 Neoproterozoic tectonic evolution of South Qinling, China: evidence from zircon
1726 ages and geochemistry of the Yaolinghe volcanic rocks. *Precambrian Research*.
1727 245, 115–130. <https://doi.org/10.1016/j.precamres.2014.02.005>
- 1728 Zhu, X.Y., Chen, F.K., Wang, W., Pham, T.H., Wang, F., Zhang, F.Q., 2008. Zircon U–
1729 Pb ages of volcanic and sedimentary rocks of the Wudang Group in the Qinling
1730 orogenic belt within Western Henan Province. *Acta Geoscientica Sinica* 29, 817–
1731 829 (in Chinese with English abstract).
- 1732 Zou, H., Li, Q., Bagas, L., Wang, X., Chen, A., Li, X., 2021. A Neoproterozoic low-
1733 $\delta^{18}\text{O}$ magmatic ring around South China: Implications for configuration and
1734 breakup of Rodinia supercontinent. *Earth and Planetary Science Letters*, 575,
1735 117196. <https://doi.org/10.1016/j.epsl.2021.117196>
- 1736
- 1737

1738 **Captions for Supplementary Figures S1 and S2**

1739 **Figure S1.** Diagram of Th/Yb vs. Ta/Yb (Pearce, 2008) for Neoproterozoic mafic
1740 igneous rocks from the north(west)ern margin of the Yangtze Block. Values for N-
1741 MORB, E-MORB and OIB are from Sun and McDonough (1989). Supplementary
1742 Table S2 for references.

1743 **Figure S2.** Nb vs Y diagram (Pearce et al., 1984) for classification of Neoproterozoic
1744 felsic magmatic rocks from the north(western) margin of the Yangtze Block. For
1745 references of data, please see Supplementary Table S2.

1746

1747 **References From the Captions of Supplementary Figures S1 and S2**

- 1748 Pearce, J.A., Harris N.B.W., Tindle, A.G., 1984. Trace Element Discrimination
1749 Diagrams for the Tectonic Interpretation of Granitic Rocks, Journal of Petrology,
1750 25, 956–983. <https://doi.org/10.1093/petrology/25.4.956>
- 1751 Pearce, J.A., 2008. Geochemical fingerprinting of oceanic basalts with applications to
1752 ophiolites classification and the search for Archean oceanic crust. Lithos 100,
1753 14–48. <https://doi.org/10.1016/j.lithos.2007.06.016>
- 1754 Sun, S.-S., McDonough, W.I., 1989. Chemical and isotopic systematics of oceanic
1755 basalts: implications for mantle composition and processes. In: Saunders, A.D.,
1756 Norry, M.J. (Eds.), Magmatism in the Ocean Basins. Special Publication.
1757 Geological Society of London, London, pp. 313– 345.
1758 <https://doi.org/10.1144/gsl.sp.1989.042.01.19>

1759

1760 **Captions for Supplementary Tables S1 to S5**

1761 **Tables S1.** Geochronology of (pre-)Neoproterozoic rocks from the northern Yangtze.

1762 **Table S2.** Whole-rock major and trace element of Neoproterozoic igneous rocks from
1763 the northern Yangtze.

1764 **Table S3.** Zircon Lu-Hf isotope compositions of Neoproterozoic igneous rocks from
1765 the northern Yangtze.

1766 **Table S4.** Zircon O isotope compositions of Neoproterozoic igneous rocks from the
1767 northern Yangtze.

1768 **Table S5.** Detrital zircon U-Pb ages and partial Hf-O isotope compositions of
1769 sedimentary rocks from the northern Yangtze.

Figure 1 to 8.

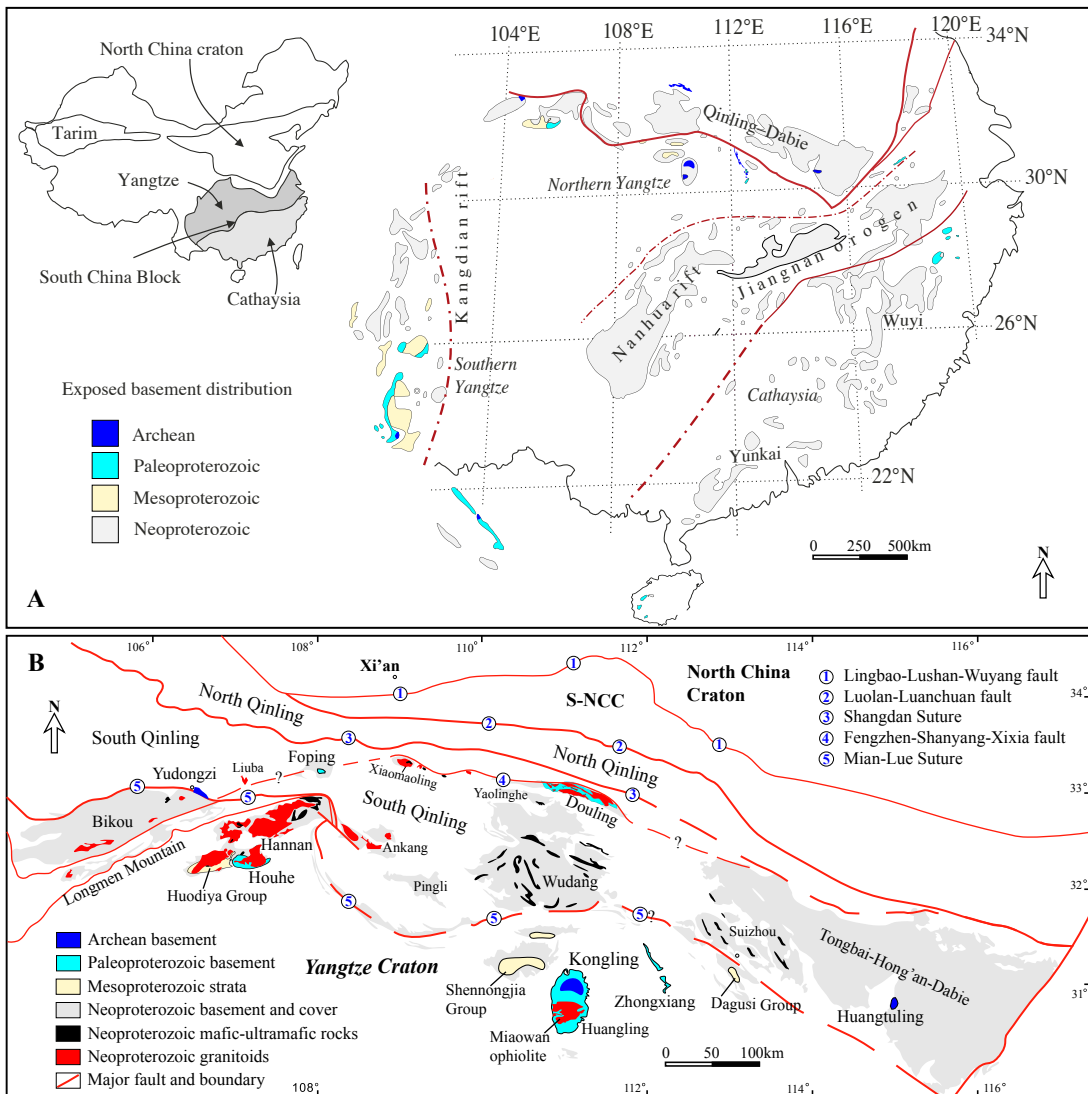


Fig. 1

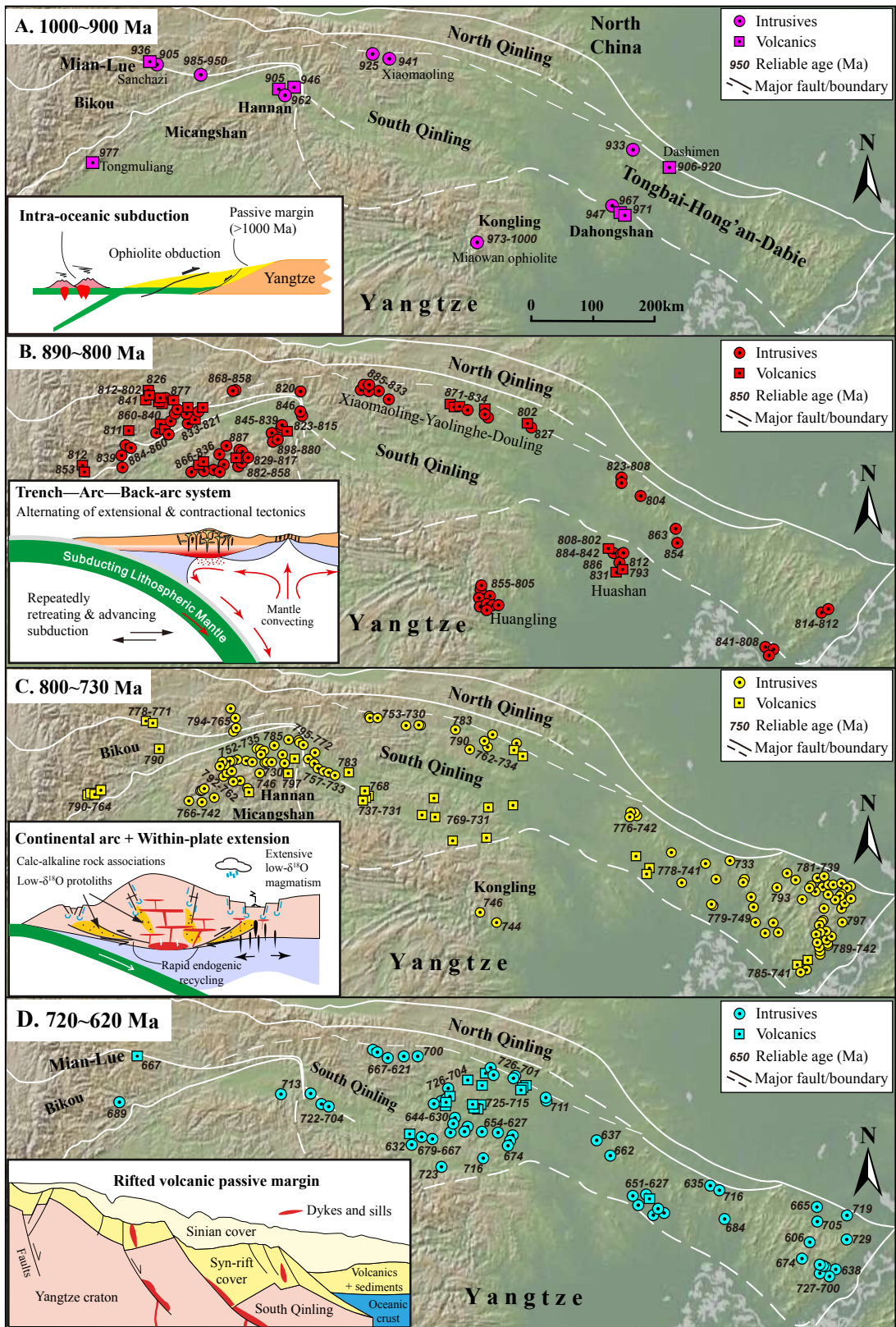


Fig. 2

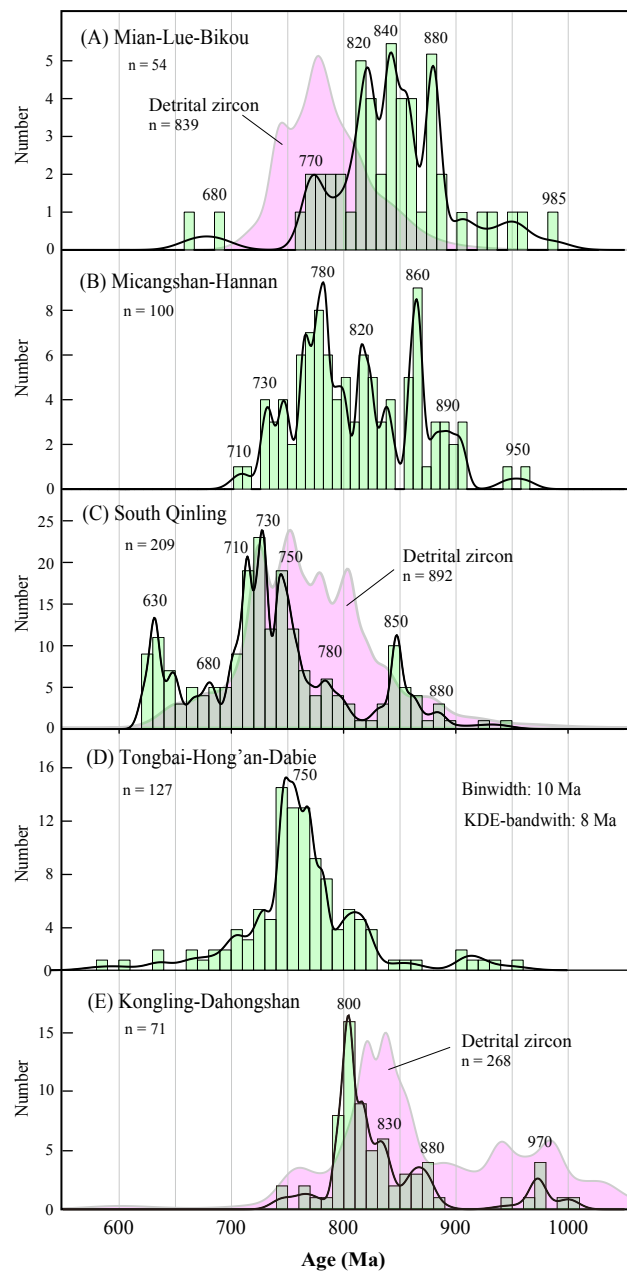


Fig. 3

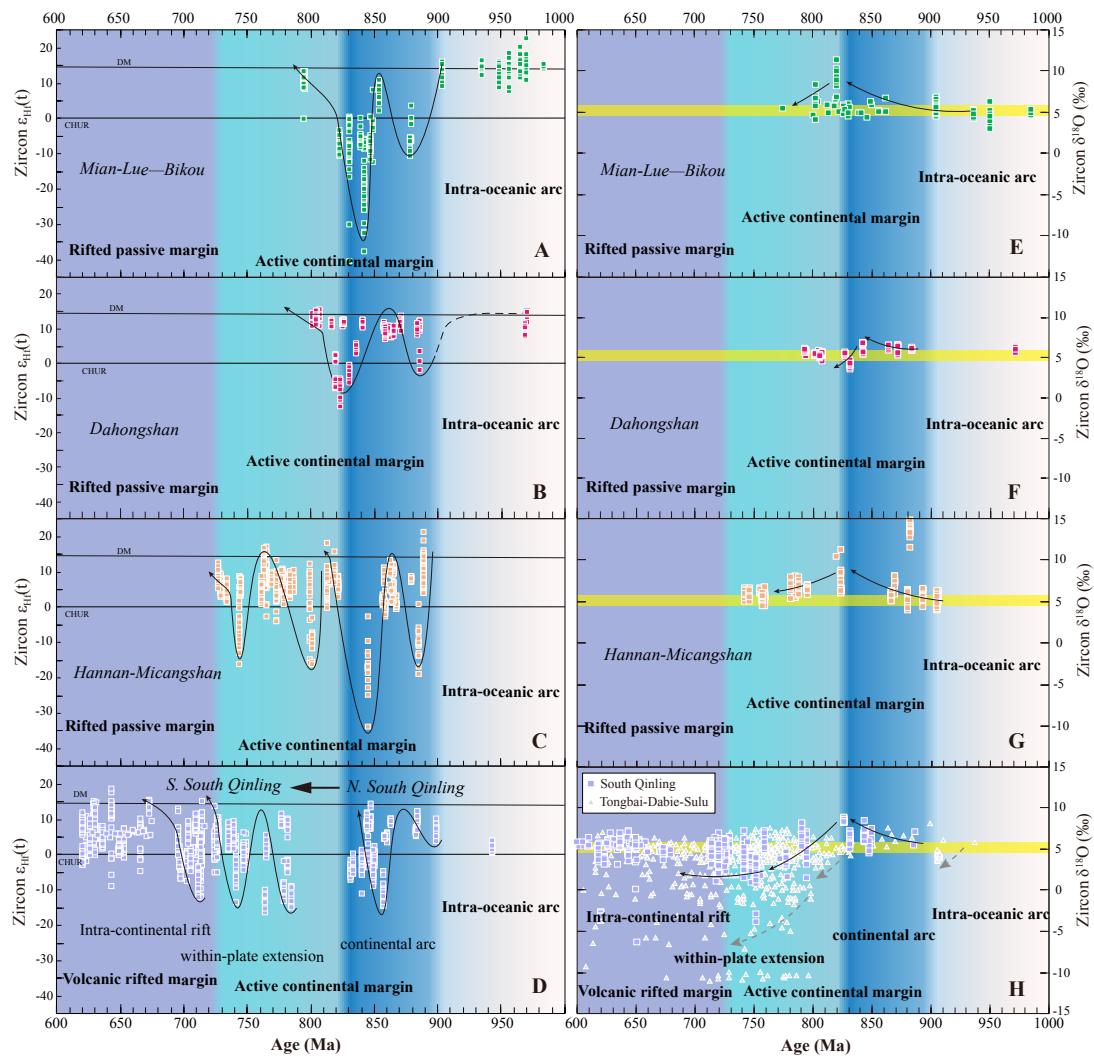


Fig. 4

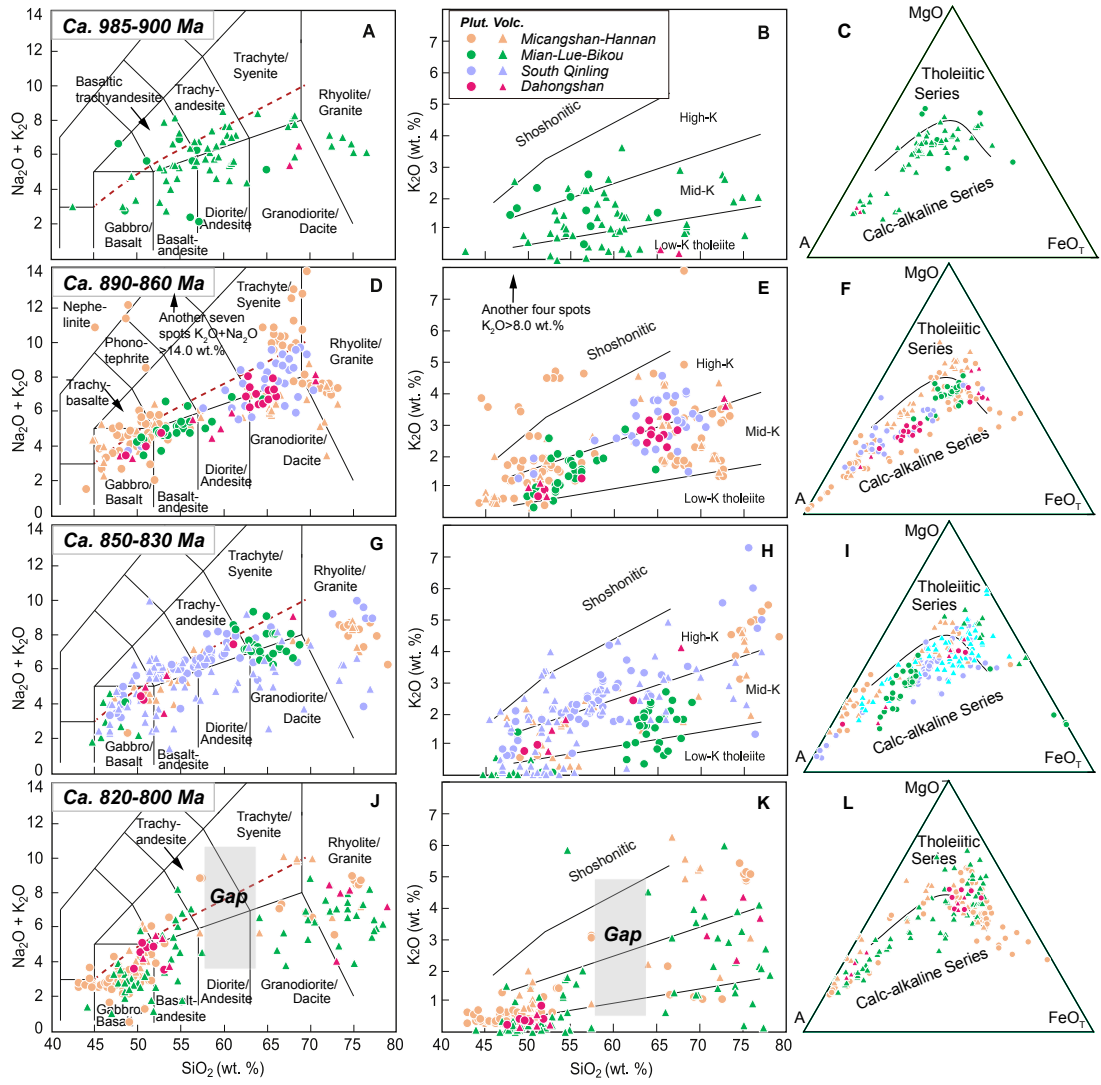


Fig. 5. (Continued)

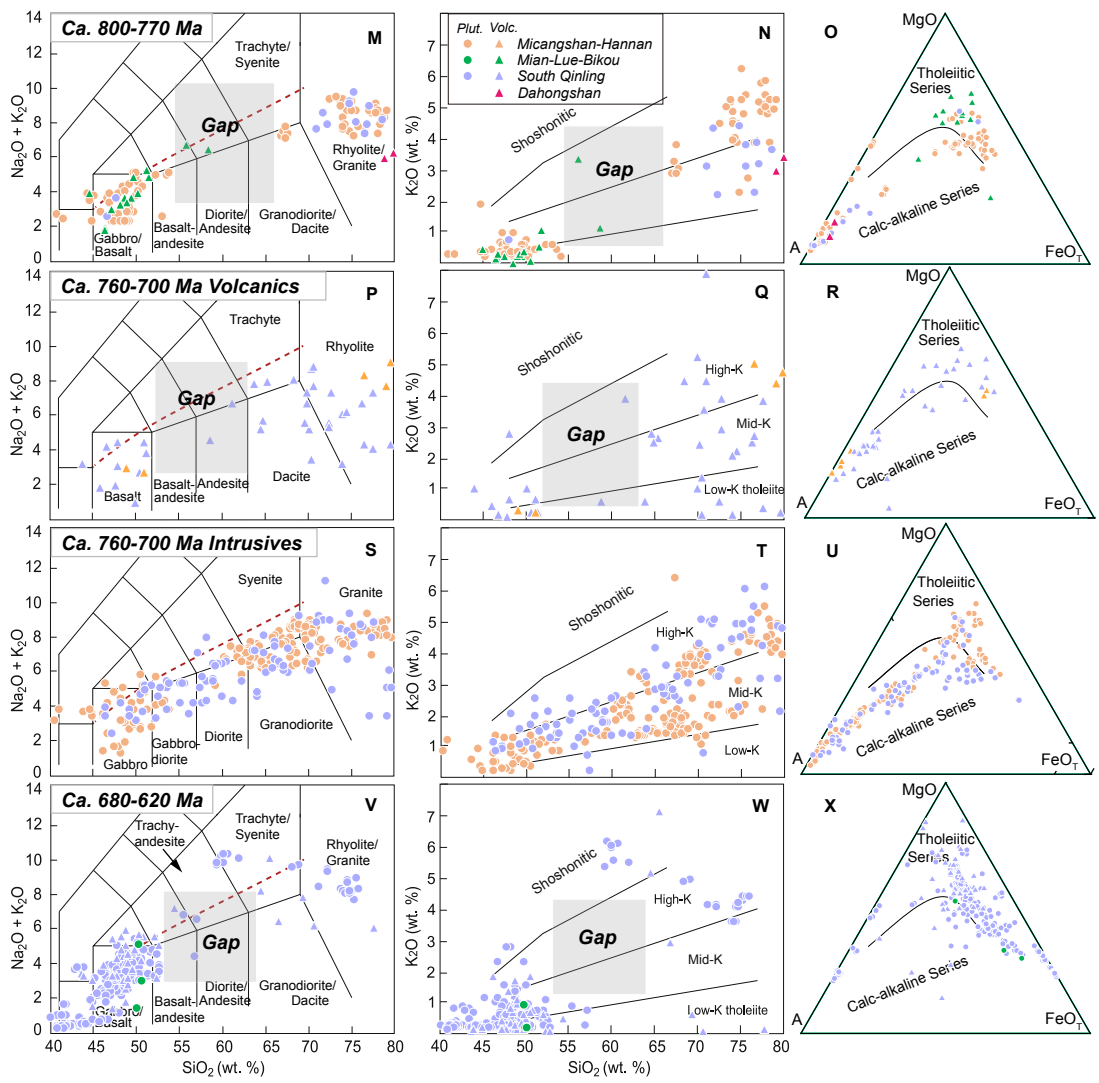


Fig. 5.

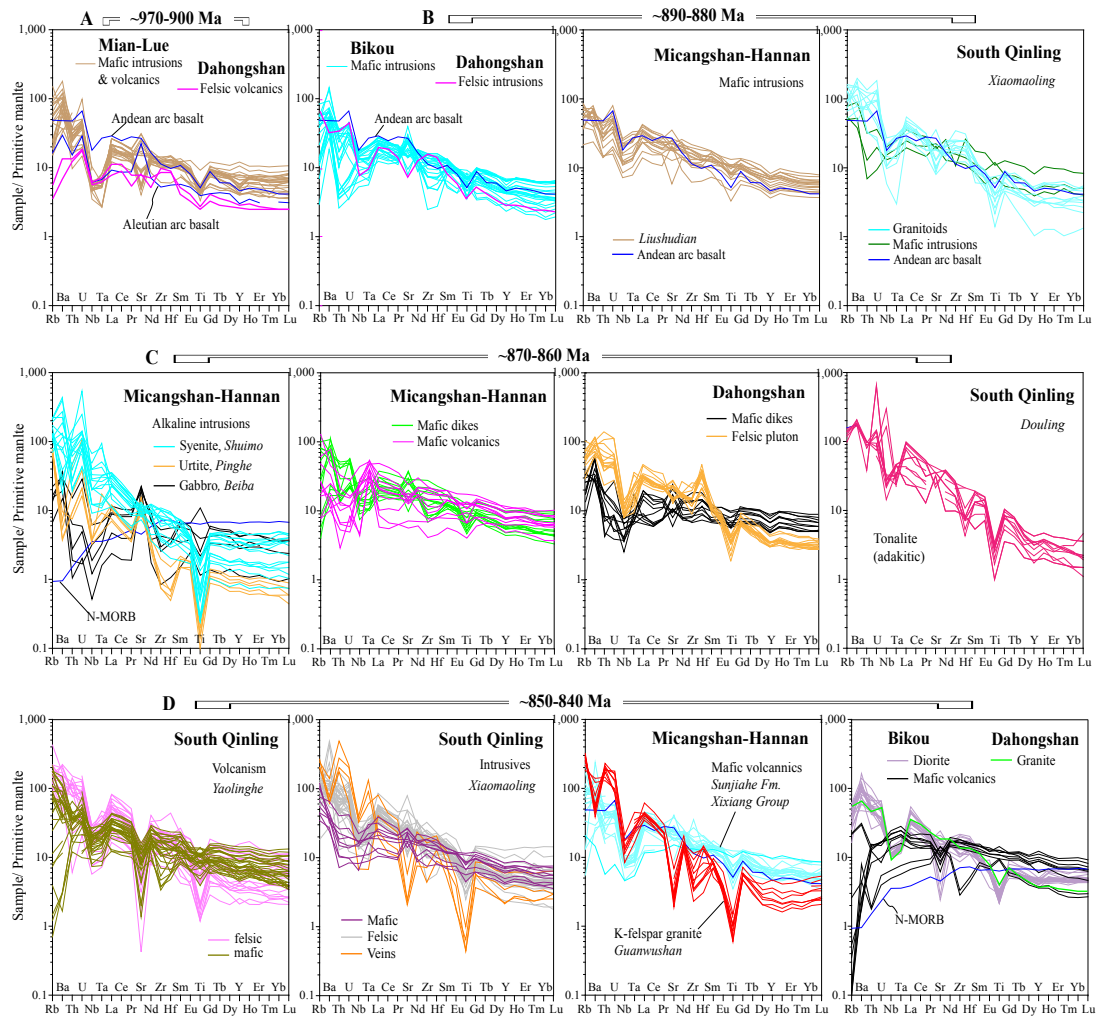


Fig. 6. (Continued)

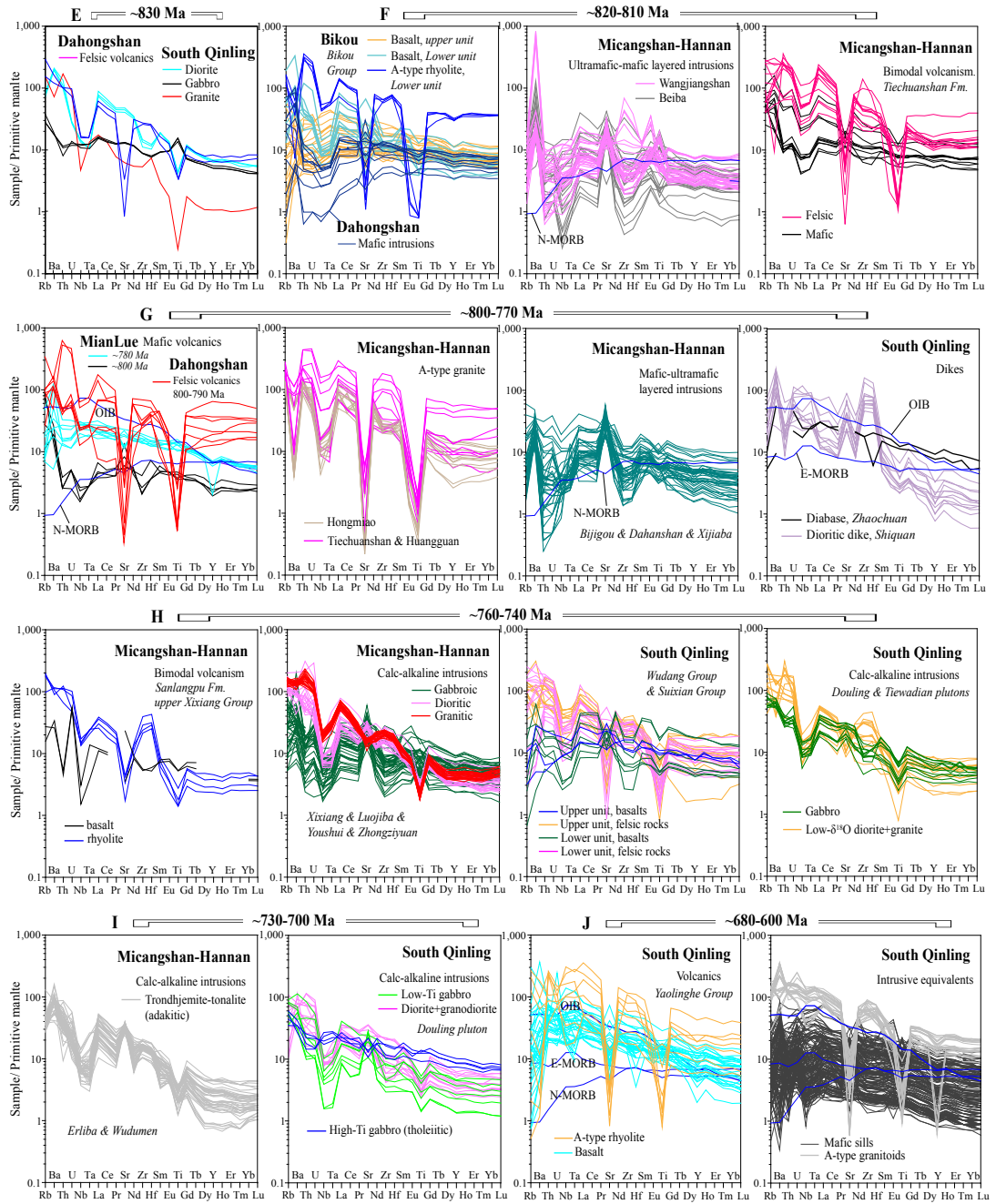


Fig. 6.

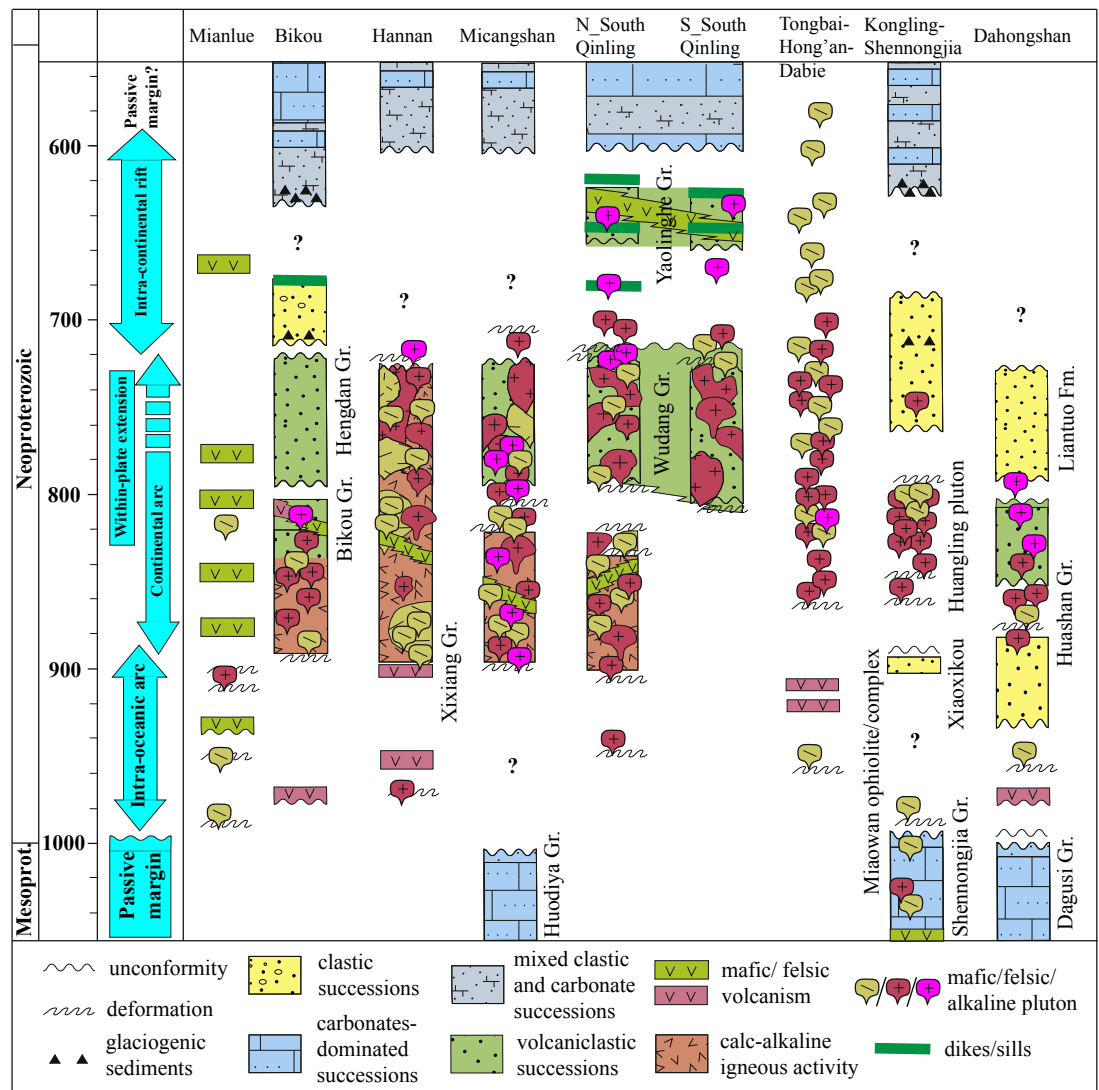


Fig. 7.

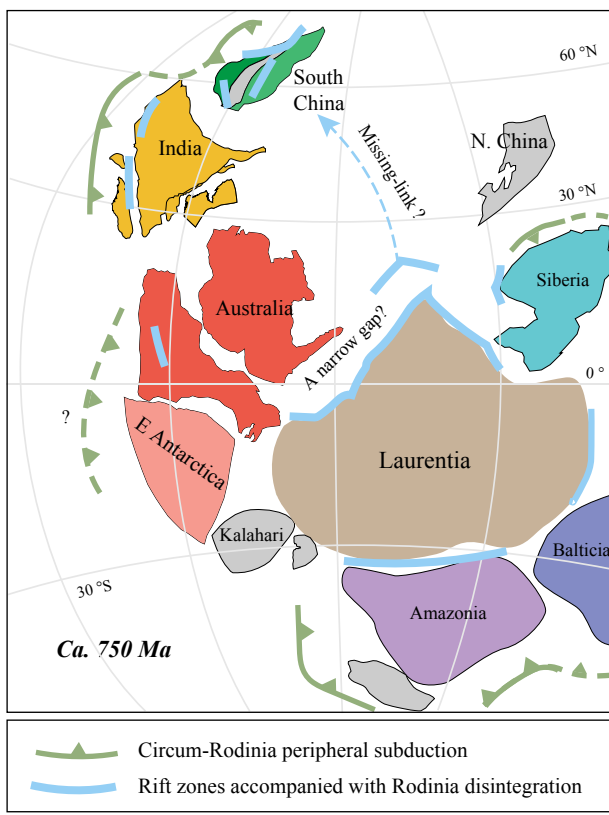


Fig. 8